OCEAN DRILLING PROGRAM

LEG 153 PRELIMINARY REPORT

MID-ATLANTIC RIDGE

Dr. Mathilde Cannat
Co-Chief Scientist, Leg 153
Laboratoire de Pétrologie
Université Pierre et Marie Curie
4 place Jussieu 75252
Paris Cedex 05
France

Dr. Jeffrey Karson
Co-Chief Scientist, Leg 153
Department of Geology
Duke University
P.O. Box 90277
Durham, North Carolina 27708
U.S.A.

Dr. D. Jay Miller
Staff Scientist, Leg 153
Ocean Drilling Program
Texas A&M University Research Park
1000 Discovery Drive
College Station, Texas 77845-9547
U.S.A.

Philip D. Rabinowitz
Director
ODP/TAMU

Jack Baldauf
Manager
Science Operations
ODP/TAMU

Timothy J.G. Francis
Deputy Director
ODP/TAMU

February 1994

Preliminary Report No. 153

First Printing 1994

Distribution

Copies of this publication may be obtained from the Director, Ocean Drilling Program, Texas A&M University Research Park, 1000 Discovery Drive, College Station, Texas 77845-9547, U.S.A. In some cases, orders for copies may require payment for postage and handling.

DISCLAIMER

This publication was prepared by the Ocean Drilling Program, Texas A&M University, as an account of work performed under the international Ocean Drilling Program, which is managed by Joint Oceanographic Institutions, Inc., under contract with the National Science Foundation. Funding for the program is provided by the following agencies:

Canada/Australia Consortium for the Ocean Drilling Program
Deutsche Forschungsgemeinschaft (Federal Republic of Germany)
Institut Français de Recherche pour l'Exploitation de la Mer (France)
Ocean Research Institute of the University of Tokyo (Japan)
National Science Foundation (United States)
Natural Environment Research Council (United Kingdom)
European Science Foundation Consortium for the Ocean Drilling Program (Belgium, Denmark, Finland, Greece, Iceland, Italy, The Netherlands, Norway, Spain, Sweden, Switzerland, and Turkey)

SCIENTIFIC REPORT

The following scientists were aboard the *JOIDES Resolution* for Leg 153 of the Ocean Drilling Program:

Mathilde Cannat, Co-Chief Scientist (Laboratoire de Pétrologie, Université Pierre et Marie Curie, 4 place Jussieu 75252, Paris Cedex 05, France. E-Mail - mac@ccr.jussieu.fr)
Jeffrey Karson, Co-Chief Scientist (Department of Geology, Duke University, P.O. Box 90277, Durham, North Carolina 27708, USA. E-mail - jkarson@rogue.geo.duke.edu)
Jay Miller, Staff Scientist (Ocean Drilling Program, Texas A&M University Research Park, 1000 Discovery Drive, College Station, Texas 77845-9547, USA. E-Mail - jaymiller@ nelson.tamu.edu)
Susan Agar (Geological Sciences Department, Northwestern University, 1847 Sheridan Road, Evanston, Illinois 60208, USA. E-Mail - agar@earth.nwu.edu)
Jane Barling (Université Libre de Bruxelles, Département des Sciences de la Terre et de L'Environnement, Av. F.D. Roosevelt, 50, C.P. 160/02, 1050 Bruxelles, Belgium)
John Casey (Department of Geosciences, University of Houston, Houston, Texas 77204, USA. E-Mail - geos55@jetson.uh.edu)
Georges Ceuleneer (OMP-UPR 234, 14, Av. Ed. Belin, 31400 Toulouse, France)
Yildirim Dilek (Department of Geology, Ely Hall, P.O. Box 205, Vassar College, Poughkeepsie, New York 12601, USA)
John Fletcher (Department of Geology and Geophysics, University of Utah, Salt Lake City, Utah 84112-1183, USA. E-Mail - jmfletch@mines.utah.edu)
Norie Fujibayashi (Faculty of Education, Department of Geology, Niigata University, 8050, Ni-no-cho, Ikarashi, Niigata, Japan. E-Mail - fujib@ed.niigata-u.ac.jp)
Laura Gaggero (Dipartimento di Scienze Terra Sezione Mineralogia-Petrografia, Corso Europa 26, I-16132 Genova, Italy. E-Mail - gaggero@HP433.dister.unige.it)
Jeffrey Gee (Lamont-Doherty Earth Observatory, Route 9W, Palisades, New York 10964, USA. E-Mail - jgee@lamont.ldgo.columbia.edu)
Stephen Hurst (Department of Geology, Duke University, 103 Old Chemistry Building, Durham, North Carolina 27708, USA. E-Mail - steve@rogue.geo.duke.edu)
Deborah Kelley (School of Oceanography, WB-10, University of Washington, Seattle, Washington 98195, USA. E-Mail - kelley@ocean.washington.edu)
Pamela Kempton (NIGL, Kingsley Dunham Centre, Keyworth, NG12 5GG, United Kingdom. E-Mail - k-pdk@nkw.va.ac.uk)
Roisin Lawrence (Department of Geology, Duke University, P.O. Box 90277, Durham, North Carolina 27708, USA. E-Mail - lawrence@rogue.duke.edu)
Vesna Marchig (Bundesanstalt für Geowissenschaften und Rohstoffe, Stilleweg 2, D30655 Hannover, Germany. E-Mail - vonrad@gate1.bgr.dbp.de)
Carolyn Mutter (Lamont-Doherty Earth Observatory, Box 1000, Palisades, New York 10964-8000, USA. E-Mail - czm@lamont.ldgo.columbia.edu)
Kiyoaki Niida (Department of Geology and Mineralogy, Faculy of Science, Hokkaido University, N-10, W-8 Kita-Ku, Sapporo, 060, Japan. E-Mail - kiyo@s1.hines.hokudai.ac.jp)
Katherine Rodway (Lamont-Doherty Earth Observatory, Palisades, New York 10964, USA. E-Mail - rodway@lamont.columbia.edu)
Kent Ross (University of Houston - TcSUH, 4800 Calhoun, Houston, Texas 77204-5932, USA)

Christopher Stephens (Department of Earth Sciences, University of Queensland, St. Lucia, QLD 4072, Australia. E-Mail - stephens@sol.earthsciences.uq.edu.au)
Carl-Dietrich Werner (Institut für Mineralogie der Bergakademie, Freiberg, Brennhausgasse 14, D-09596 Freiberg, Germany)
Hubert Whitechurch (École et Observatoire de Physique de Globe (IPG) de Strasbourg, 5 rue René Descartes, 67084 Strasbourg Cedex, France)

ABSTRACT

The principal success of Leg 153 was the recovery of extensive sections of ultramafic and mafic rocks from a slow-spreading mid-ocean ridge. Drilling was undertaken at multiple sites along the western flank of the Mid-Atlantic Ridge (MAR), south of the Kane Transform (MARK). The principal objectives of this second in a series of offset drilling legs and subsequent shore-based studies were to investigate the chemical composition and evolution of the lower crust and mantle created at a slow-spreading ridge, the geometry of magmatic and deformation structures preserved in residual peridotite and in lower crustal rocks, and the intensity and diversity of metamorphism attending crustal evolution in this slow-spreading environment.

Site 920, located at latitude 23°20.32'N, about 40 km south of the Kane Transform along the western wall of the Mid-Atlantic Ridge median valley, sampled predominantly serpentinized harzburgite, interpreted to represent uplifted and altered suboceanic mantle. Drilling at this site achieved the best penetration and recovery of any drilling efforts to date in massive serpentinized peridotite. Other rock types sampled from this site include serpentinized lherzolite, dunite, clinopyroxenite, and websterite, as well as variably metamorphosed intervals of gabbro, olivine gabbro, oxide mineral-rich gabbro and gabbronorite, and plagioclase-olivine phyric diabase. Despite intense alteration of the primary minerals to serpentine, primary mineralogy and textures are widely preserved in the recovered ultramafic rocks. The dominant texture is coarse grained porphyroclastic with lobate grain boundaries and frequent 120° triple junctions, suggesting efficient grain growth at close to solidus temperature. Most samples also display an anastomosing serpentine foliation that results from the preferred orientation of fine, discontinuous veins of serpentine and iron oxide minerals cutting the background mesh-textured serpentine. Paleomagnetic studies indicate that this anastomosing foliation probably dips moderately to the east, toward the MAR neovolcanic zone. Pyroxenite and gabbroic veins, and gabbroic intervals up to at least a few decimeters thick are ubiquitous in the cored ultramafic rocks, and cover a wide range of compositions from spinel-bearing interstitial melt segregations to altered, oxide mineral-, apatite-, and zircon-bearing gabbro.

Sites 921 through 924 are located in outcrops of gabbroic rocks, also along the western wall of the Mid-Atlantic Ridge median valley near its intersection with the Kane Transform. These outcrops occur on the flank of a broad, dome-like uplift, referred to as an inside-corner high or

ridge/transform intersection massif. Sites 921, 922, and 923 lie along a north-south-trending ridge axis parallel transect, such that variations in the igneous, metamorphic, and deformational features in the rocks recovered from these sites may reflect along-axis variability in the processes that create and modify lower crustal rocks. Site 924 is offset toward the MAR and may therefore, assuming a simple, symmetrical spreading history, have sampled younger gabbroic rocks. Lithologies recovered from this series of holes are predominantly gabbro and olivine gabbro, with lesser volumes of troctolite, oxide mineral-rich gabbro, trondhjemite, and diabase. The recovered gabbroic rocks are characterized by a wide range of compositional and textural variability over length scales of a few centimeters to a few tens of meters. Igneous layering is commonly observed and occurs as changes in grain size or modal mineralogy. Crystal-plastic deformation is also common and is concentrated in centimeter- to decimeter-scale shear zones with dominantly normal displacements. Brittle deformation occurs in centimeter- to decimeter-scale cataclastic shear zones, which are likely to be associated with the east-dipping fault surfaces seen in the surrounding outcrops.

INTRODUCTION

Accretion of oceanic lithosphere along the mid-ocean-ridge system is a first-order tectonic process on Earth. Approximately 70% of the Earth's present lithosphere was created at mid-ocean-ridge spreading centers through the interplay of magmatic construction, mechanical extension, and hydrothermal alteration. Since the inception of plate tectonics, a vast volume of oceanic lithosphere has been produced at spreading centers, then recycled back into the mantle at subduction zones. Despite this global significance of oceanic lithosphere, the understanding of its detailed internal structure, constitution, and modes of creation are limited.

In the past 2 decades, extensive studies of the morphology and surficial geology of mid-ocean-ridge spreading centers have been conducted. Samples of coarse-grained mafic and ultramafic rocks, which are thought to have formed in the middle to lower crust and in the upper mantle beneath spreading axes, have been sampled from seafloor outcrops, but the geologic setting and vertical dimensions of these rock bodies are poorly constrained. Indirect seismic investigations of oceanic crust and studies of ophiolite complexes, considered to be on-land exposures of oceanic crust and upper mantle, provide the foundation of our understanding of the deeper levels of the oceanic crust and upper mantle. The Deep Sea Drilling Project (DSDP) and Ocean Drilling

Program (ODP) have made the investigation of the oceanic lithosphere a high-priority thematic objective, following the recommendations of the Conferences on Scientific Drilling (COSOD I and II reports).

Drilling the hard-rock foundation of the ocean floor has proven to be very difficult due to the drilling problems posed by the highly fractured nature of the basaltic carapace that typically characterizes surface exposures. However, success in drilling plutonic rocks exposed in locations where the oceanic crust has been stripped of its overlying fine-grained basaltic cover on Legs 109 and 118, led to development of a strategy for drilling a series of relatively shallow, closely spaced holes that can be correlated laterally (offset drilling). The report of the Offset Drilling Working Group recommended a program directed toward collecting continuous sections of deep crustal rocks that could be used to erect composite sections of the oceanic crust created in various spreading environments.

The first holes of this program were drilled during Leg 147 in the walls of the Hess Deep Rift of the Equatorial Pacific. This exposure of the plutonic foundation of 1-Ma crust formed at the fast-spreading (132 mm/yr) East Pacific Rise is the result of amagmatic rifting at the westward-propagating tip of the Cocos-Nazca plate boundary. Drilling at two nearby sites yielded substantial sections of coarse-grained gabbroic and serpentinized ultramafic rocks, the most extensive suite of samples collected to date of deep crustal and upper mantle rocks created at a fast-spreading ridge.

Leg 153 represents a second ODP offset drilling leg, in this case devoted to drilling the plutonic foundation of slow-spreading (~25 mm/yr) oceanic lithosphere in the MARK area (Mid-Atlantic Ridge at the Kane Transform). Coarse-grained mafic and ultramafic rocks are exposed on the MAR median valley walls in this region and are estimated to be <1 Ma. These exposures are considered to have resulted from mechanical extension of the axial lithosphere during a period of limited magmatic construction. Site 920 and Sites 921 to 924, drilled during Leg 153, are located in the footwalls of major detachment faults cutting ultramafic and gabbroic rocks, respectively.

The primary goals of Leg 153 included the investigations of the mantle flow and partial melting history of the ultramafic rocks, the igneous history of the gabbroic rocks, and the deformation and metamorphism attending seafloor spreading in this slow-spreading environment. Of particular interest also was the study of the possible interplay between igneous and deformational processes, both in the ultramafic rocks and in the gabbroic rocks. It was anticipated that the ultramafic rocks would yield information on mantle flow under both asthenospheric and lithospheric conditions; on melt generation, segregation, and transport within residual upper mantle material beneath the ridge axis; and on high- to low-temperature hydration and deformation of ultramafic rocks along fault zones associated with seafloor spreading. Studies of gabbroic rocks were expected to reveal the igneous evolution of melts that reside in the middle to lower crust and the retrograde deformation and hydrothermal alteration associated with major oceanic fault zones. The relative timing and spatial distribution of igneous and deformational episodes in both the ultramafic and gabbroic rocks were also anticipated to help constrain the interplay of tectonism and magmatism in presumably magma-poor, slow-spreading environments. Drilled samples are unique in that they provide the potential to investigate the details of magmatic evolution on the scale of centimeters to meters, to document the dimensions of plutonic bodies and the nature of contacts between different igneous rock types. Substantial volumes of various rock types also permit a range of geochemical and petrological investigations. Likewise, structural and metamorphic studies involving textural and mineralogical changes that take place over centimeters and meters can be made.

Detailed paleomagnetic and other physical properties studies of these rock types were expected to shed light on the magnetic, gravity, and seismic expressions of the oceanic crust and upper mantle. Finally, it was anticipated that structures found in cores could be reoriented with respect to geographic coordinates, based on paleomagnetic and logging results, allowing them to be evaluated in the context of the slow-spreading ridge axis and outcrop-scale features previously mapped by camera sleds and manned submersibles in the MARK area.

GEOLOGICAL BACKGROUND

The Mid-Atlantic Ridge near latitude 23°N and the Kane Fracture Zone, known as the MARK area (Fig. 1), is the most comprehensively studied portion of the MAR. Investigations in the area date back to initial conventional wide-beam echo-sounding surveys and dredging in the late 1960's (Miyashiro et al., 1969, 1970; van Andel et al., 1969; Fox, 1972). These and subsequent geological and geophysical studies (Table 1) demonstrated the general character of the ridge in this area and the diverse rock types that are exposed in the median valley and transform-fault walls.

A SeaBeam map of the MARK area was produced during the site survey for Leg 106 (Detrick et al., 1984). This map has served as the base map for all subsequent studies and has been the basis for morphological and large-scale structural investigations (Kong et al., 1988; Pockalny et al., 1988). Magnetic data also collected during the Leg 106 site survey were interpreted by Schulz et al. (1988). The off-axis distribution of magnetic-anomaly lineations indicates asymmetrical spreading with about 14.1 mm/yr to the west and 11.3 mm/yr to the east. Possible duplication of anomalies to the west suggests that discrete eastward ridge jumps also may have occurred.

For nearly 200 km south of the Kane Transform, the MAR is relatively linear and has no major transform offsets. The floor of the rift valley (below 3500 m depth) varies in width from 14 to 20 km, with relief ranging from less than 1 to more than 4 km from the valley floor to the adjacent crestal mountains. In general, the inner floor deepens and broadens toward the north from <3500 mbsl near the saddle at latitude 22°55'N to >6100 mbsl in the nodal basin marking the intersection with the Kane Fracture Zone (Fig. 1).

Superimposed on this regional pattern are a series of discrete spreading segments or spreading cells that are defined on the basis of their morphology, geological character, and geophysical characteristics. Gravity data obtained along the MAR axis suggest that such segments, which are typically a few tens of kilometers long, may result from a focusing of the ridge's magma supply beneath segment centers, with attenuation of magmatism near the segment ends (Kuo and Forsyth, 1988; Lin et al., 1990; Patriat et al., 1991; Deplus et al., 1992). The MARK area comprises a series of such segments, which have been distinguished based on ridge-axis morphology and tectonics (Karson et al., 1987; Kong et al., 1988), seismic studies (Purdy and Detrick, 1986), and gravimetry (Morris and Detrick, 1991).

The northernmost segment (Cell 1, Fig. 1), extending from the Kane Fracture Zone nodal basin southward to about 23°18'N, displays widespread exposure of gabbroic and ultramafic rocks. These rocks are interpreted as exposures of upper mantle and lower crust material that have been unroofed by extensional tectonics, probably during periods of spreading with very limited magmatic construction. Regional geochemical studies indicate that this entire portion of the MAR is characterized by relatively depleted upper mantle and low degrees of mantle melting (Juteau et al., 1990; Komor et al., 1990). The northern ridge segment also has a continuous neovolcanic ridge, on top of which lies the Snake Pit hydrothermal field (ODP Leg 106 Scientific Party, 1986; Site 649; Fig. 1).

The next ridge segment to the south (Cell 2, Fig. 1)is located at a local high point along the ridge axis. Near the center of this segment lies Serocki Volcano, (ODP Leg 106 Scientific Party, 1986; Site 648). The boundary between the two segments is a relatively wide transition zone (extending from 23°18'N to 23°05'N) which corresponds with both a probable offset of magnetic anomalies (Schulz et al., 1988) and a marked change of rift-valley morphology (Karson et al., 1987; Kong et al., 1988). It has been interpreted as a zero-offset transform fault (Purdy and Detrick, 1986) or as an accommodation zone linking two regions of different spreading styles (Brown and Karson, 1988).

Results of an off-axis swath mapping and gravity survey (Gente et al, 1991; Deplus et al., 1992) suggest that this accommodation zone or zero-offset transform can be traced into lithosphere of 4 to 5 Ma, and is characterized by greater than average bottom depth and positive residual mantle Bouguer anomalies. These observations suggest that this lineament is underlain by relatively thin crust. Most serpentinized peridotite outcrops in the MARK median valley wall, off-axis dredges of serpentinized peridotite (Cannat et al., 1993), and DSDP Site 395 (where serpentinite-bearing breccias were drilled close to the surface) are all located within this domain of inferred thin crust. Along-axis (Morris and Detrick, 1991) and off-axis (Deplus et al., 1992) gravity studies in the northern ridge segment suggest that thin crust has also been accreted there during the past 4 to 5 m.y. This is consistent with the interpretation of geological observations made in this segment in terms of tectonically dominated spreading in a magma-poor spreading environment (Karson et al., 1987; Karson, 1991, Mével et al., 1991).

The sites drilled during Leg 153 are all located on the western wall of the median valley, in the northern ridge segment (Fig. 1). Site 920, where serpentinized ultramafic rocks were drilled, lies at 23°20.32'N, at the southern end of this segment. Sites 921 through 924, where gabbroic rocks have been drilled, lie between 23°31.36'N and 23°32.55'N, 8 to 12 km south of the Kane Fracture Zone.

RESULTS

Site 920

Drilling Serpentinized Ultramafic Rocks in the MAR Median Valley Wall

Site 920 is located on the western median valley wall of the Mid-Atlantic Ridge at 23°20.32'N, about 40 km south of the Kane Transform. It is set in an extensive body of serpentinized peridotite that is exposed in a 2-km-wide belt that extends parallel to the MAR axis for at least 20 km (Karson et al., 1987). Drilling at Site 920 achieved the best total penetration and recovery of any hard-rock drilling efforts to date in massive serpentinized peridotite, and even preliminary studies have provided an exciting glimpse of processes that operate beneath slow-spreading mid-ocean ridges.

Serpentinite outcrops on the western median valley wall of the MARK area were discovered during a series of *Alvin* dives (Karson et al., 1987) and were subsequently explored by *Nautile* dives (Mével et al., 1991) and dredge operations (Gente et al., 1989). The last 4 days of Leg 109 were devoted to unsupported drilling at ODP Site 670 in the southern part of the serpentinite body. Penetration rates were good, and a depth of nearly 100 mbsf was reached, but recovery rates were poor (only 7% cumulative recovery). Serpentinized harzburgite and lherzolite, with rare intervals of dunite and pyroxenite, were cored.

Site 920 is located on the median valley wall along one of the *Nautile* dive tracks, in the northern part of the serpentinite body (Figs. 1 and 2). In this area, the summit of the rift-valley wall culminates at a depth of 2600 mbsl. Pillow basalts crop out at the top of the slope, above 3100 mbsl. The relatively young, fissured pillow basalts of the median valley floor abut the base of the rift-valley wall at about 3700 m depth. The base of the slope is covered by talus of serpentinite blocks and basalt fragments.

Serpentinized ultramafic rocks crop out nearly continuously from about 3500 mbsl to about 3100 mbsl. This portion of the median valley wall is a tectonically active slope, dominated by east-facing, presumably normal, faults with relatively steep dips (40° to 70°), cutting a more pervasive, gently east-dipping (20° to 40°) schistosity, which is thought to be related to earlier, low-angle faults and shear zones. Ultramafic rocks sampled during *Nautile* dives HS 13 and HS 19

(Fig. 2) show serpentinite shear zones and veins oriented approximately parallel to a crystal-plastic fabric defined by elongated pyroxene grains (Mével et al., 1991). Site 920 is located at a depth of 3340 mbsl (Fig. 3), on a flat terrace covered by a smooth blanket of pelagic ooze and rubble, which overlies massive outcrops of slabby and schistose ultramafic rocks.

The four holes drilled at Site 920 met with different degrees of success. Only 1.5 m of mixed basaltic, gabbroic, and ultramafic rubble and serpentinized peridotite was recovered from Hole 920A, and there was no recovery from Hole 920C. Holes 920B and D reached depths of 126 and 200 m respectively, and recovered a total of 144.5 m of serpentinized peridotite and lesser, variably deformed and metamorphosed mafic rocks. Cumulative recovery was 38% from Hole 920B (Fig. 4), where seven rock units were identified, and 47% from Hole 920D, with 13 rock units. The following summary is based upon the preliminary results of igneous, metamorphic, structural, paleomagnetic, and physical-properties studies of cores from these two holes. These two holes are only 20 m apart, and several units appear to be present in both cores. Still, subtle to very obvious differences between the cores document the significant heterogeneity over this short lateral distance and give a sense of the compositional and textural variations that are present in this crustal volume. Continuing studies of this unique sample set will provide significant new insights into the melting regime beneath mid-ocean-ridge axes, the architecture of serpentinite bodies in the upper oceanic crust, and the mode of unroofing of these anomalous, exposed masses of modified upper-mantle material.

The predominant rock types recovered at Site 920 are serpentinized harzburgite, with lesser amounts of lherzolite, dunite, clinopyroxenite, and websterite along with variably altered olivine gabbro, gabbro, oxide-rich metagabbro, oxide-rich gabbronorite, oxide-rich clinopyroxenite, amphibolitized microgabbro, amphibolite, hornblendite, rodingitized gabbro, and plagioclase-olivine phyric diabase. Despite the typical intense alteration of the primary minerals to serpentine, primary mineralogy and textures are widely preserved.

Ultramafic rock units sampled at Site 920 include dominantly massive harzburgite with locally interlayered pyroxene-rich (up to 35% orthopyroxene) and pyroxene-poor harzburgite to dunite (Fig. 5). Layer thicknesses range from a few meters to a few centimeters. Coarse-grained porphyroclastic textures are nearly ubiquitous, with large (4-10 mm) orthopyroxene porphyroclasts surrounded by orthopyroxene and olivine neoblasts, which are typically on the order of 1 mm in size. Clinopyroxene (<5%) and chrome spinel (~1%) are also present. Lobate grain boundaries and numerous 120° triple junctions suggest efficient grain growth at close to solidus temperatures.

Of special interest are numerous elongated segregations or veins of spinel, clinopyroxene, plagioclase, or a combination of these phases, in the serpentinized ultramafic rocks. These range from linked, cuspate aggregates of spinel or clinopyroxene that appear to be distributed along grain boundaries and at multiple grain contact points of the peridotite, to gabbroic layers up to at least a few centimeters thick. Examples of veins and segregations that are concordant and discordant with respect to the dominant deformation fabrics are observed. Some of these segregations are bounded by symmetrical, parallel bands of pyroxene-poor harzburgite to dunite. They are interpreted as the crystallization products of interstitial melt channels in the ultramafic rocks.

Numerous veins of an altered gabbroic composition, containing zircon, apatite, brown amphibole, and oxide minerals as accessory phases, are also found in the cored ultramafic rocks. These veins are highly altered to amphibole and chlorite, with rare relics of igneous plagioclase and pyroxene. These segregations and veins are interpreted to be the crystallization products of liquids derived from interstitial melt channels, which precipitated when the liquids encountered more open conduit conditions.

The primary igneous mineralogy of the rocks is pervasively altered, typically to about 80% secondary phases. These include mainly serpentine with lesser tremolite-actinolite, chlorite, magnetite, and carbonate minerals, reflecting pervasive low-temperature (greenschist facies) metamorphism. Locally, remnants of cummingtonite and talc suggest that a higher temperature event may also have affected these units. Multiple generations of serpentine veins record a history of progressive alteration and volumetric expansion in the serpentinites. Pyroxene- and/or plagioclase-bearing melt channels range from fresh to highly altered with extensive replacement by tremolite-actinolite, chlorite, secondary plagioclase, and magnetite.

Deformation features bear witness to a complex strain history at progressively decreasing temperature conditions. With the exception of a few high-temperature shear zones, typically 10 to 20 cm wide, crystal-plastic foliation defined by weakly to moderately elongated pyroxene porphyroclasts and domains of recrystallized olivine and pyroxene, is remarkably constant through the cores. These early, high-temperature features are overprinted in most samples by an anastomosing serpentine foliation that is highlighted by thin, white serpentine veins. This serpentine foliation results from the preferred orientation of fine, discontinuous veins of serpentine, and serpentine and iron oxide minerals cutting the background mesh-textured serpentine. Evidence for shearing along this fabric is rare. It is cut by multiple generations of serpentine-bearing veins.

Coarse-grained gabbroic intervals, on the order of a few tens of centimeters thick, are interspersed within the serpentinized harzburgite. They are pegmatitic to medium-grained metagabbro and oxide mineral-bearing metagabbro, which display various degrees of deformation and metamorphism. Some of these gabbroic intervals have been pervasively deformed at granulite to amphibolite facies conditions. These contain pervasively recrystallized brown amphibole, calcic plagioclase, clinopyroxene, and olivine and have strong linear and/or planar fabrics. One oxide gabbro interval in Hole 920B has been highly deformed to produce a porphyroclastic mylonite. Lower temperature greenschist-facies mineral assemblages partially replace the high-temperature mineralogy of these gabbroic intervals, and one sample is partially rodingitized. Prehnite and zeolite veins are common in these lithologies.

A diabase dike with partially preserved chilled margins cuts the serpentinized harzburgite in both Holes 920B and D. In addition to this diabase, several other distinctive mafic and ultramafic rock units have been tentatively correlated between the two holes.

Paleomagnetic studies on half-core and minicore samples have been used to document the magnetic properties of the various rock types recovered. The serpentinized harzburgite has very high natural remanence (mean 11.8 ± 4.9 A/m) and susceptibility (0.01-0.1 SI). Strong susceptibility anisotropy appears to be the result of magnetite concentrations, which commonly parallel the anastomosing serpentine foliation. The measured inclination is similar to the present field for this location, and therefore the orientations of various structures in the core may be at least partially corrected. Assuming that the paleomagnetic declination matches the expected dipole direction, it appears that the anastomosing serpentine foliation in Holes 920B and D dips dominantly to the east (Fig. 6), toward the Mid-Atlantic Ridge axis.

The cored ultramafic rocks have bulk densities ranging from 2.58 to 3.04 g/cm^3, with a mean value of 2.66 g/cm^3. Porosity is locally high, ranging from 1.18% to 10.35%, with a mean value of 3.96%. Compressional wave velocities, measured at 1 atm, in the ultramafic rocks range from 3.65 to 5.21 km/s (mean value of 4.39 km/s). Electrical resistivity and thermal conductivity also have been documented for the major rock units recovered. These preliminary physical-properties results show good correlations with the rock types and degree of alteration.

Sites 921, 922, 923, and 924

Drilling Gabbroic Rocks in the MAR/Kane Transform Intersection Massif

Sites 921, 922, 923, and 924 are located in extensive exposures of gabbroic rocks, on the west wall of the MAR median valley near its intersection with the Kane Fracture Zone (Figs. 1 and 7). In this area, the western median-valley wall forms a broad, dome-like uplift on the order of 20 km across. It is bounded to the north by the Kane Transform and to the east by the median valley of the MAR. This is referred to as an inside-corner high or ridge/transform intersection massif. The opposing median-valley wall on the east side of this ridge segment is substantially deeper (~3500 m), less steep, and has exposures of only block-faulted basaltic pillow lavas.

Dredges (Miyashiro et al., 1969, 1971), *Alvin* dives (Dick et al., 1981; Karson and Dick, 1983; Karson et al., 1987), and *Nautile* dives (Mével et al., 1991; Auzende et al., 1993) along the east and north-facing slopes of the ridge/transform intersection massif have documented extensive outcrops of gabbro, metagabbro, metabasalt, and metadiabase, and lesser serpentinized peridotite. Samples from these outcrops commonly display slickensides, shear zones, or schistosity. The outcrops are marked by moderately dipping faults and shear zones defining a nearly continuous dip slope. Some fault zones can be followed for several hundred meters upslope and may correspond to major detachment faults (Dick et al., 1981; Karson and Dick, 1983; Karson, 1991; Mével et al., 1991). They dip to the east-northeast along the eastern face of the massif and to the north and northeast along the northern, transform-parallel wall. These gently dipping fault zones are commonly cut by higher angle faults that impart a stepped pattern to the edges of the massif. Faults on the eastern side are normal faults, whereas faults with moderately to gently plunging striae occur along the transform valley wall. The summit of the massif is covered with highly fractured and degraded basaltic rocks.

The gabbroic samples dredged and collected during submersible dives from the intersection massif include variably deformed and metamorphosed olivine gabbro to gabbronorite as well as more highly evolved ferrogabbro to trondhjemite (Karson and Dick, 1983; Mével et al., 1991; Marion et al., 1991; Marion, 1993). Deformation structures range from brittle to ductile, and metamorphic assemblages indicate alteration by magmatic fluids (Kelley and Delaney, 1987) and seawater penetration and hydrothermal alteration from amphibolite to below greenschist-facies conditions (Delaney et al., 1985; Marion et al., 1991; Marion, 1993; Kelley et al., 1993; Gillis et al., 1993).

Sites 921, 922, 923, and 924 are located on the upper eastern slopes of the intersection massif, close to the tracks of *Nautile* and *Alvin* dives (Fig. 7). Each hole drilled at these sites was drilled directly on top, or just a few meters above, outcrops of slabby to schistose gabbroic rocks, with east-dipping platy surfaces typical of those described from submersible studies in the area. These surfaces are interpreted as dip slopes on fault surfaces and shear zones. Holes at Sites 921 (23°32.40'N, 45°01.85'W) and 923 (23°32.556'N, 45°01.897'W) lie within 240 m of one another, at depths of 2440 to 2514 mbsl (Fig. 8). Site 922 is located about 2 km south of Site 921 at 23°31.37'N, 45°01.93'W, and 2612 mbsl. Site 924 lies at 23°32.47'N, 45°0.88'W, and 3176 mbsl, 1.7 km east and downslope from Sites 921 and 923 (Fig. 7). Sites 921, 922, and 923 lie along a north-south, ridge-parallel transect across the flank of the gabbro massif. Variations in igneous, deformational, and metamorphic features in the rocks recovered from these holes may therefore reflect along-axis variability in the processes that create and modify lower crustal rocks. Site 924 is closer to the MAR axis, and therefore, assuming the simplest, symmetrical spreading history, the rocks recovered from this site might be as much as 100,000 yr younger than those from Sites 921, 922, and 923. Thus, it is possible that variations in the character of the rocks recovered from these sites reflect temporal variations in spreading processes.

A total of 120 m of gabbroic rocks was recovered at Sites 921, 922, 923, and 924, from coring 447 m of hole (26.8% cumulative recovery). Hole 923A, the only hole at this site, penetrated to a depth of 70 mbsf, with a cumulative recovery rate of 58.2% (79% in the lower 50 m; Fig. 9). This high recovery provides the best record of downhole igneous, deformational, and metamorphic variability in the gabbroic rocks, at scales of a few centimeters to a few tens of meters. Hole 921E had the deepest penetration (82.6 mbsf; 21.4% cumulative recovery). It also provides valuable information on downhole variations.

The most striking characteristic common to all the gabbroic rocks drilled during Leg 153 is the wide range of compositional and textural variability they display over length scales of a few centimeters to a few tens of meters. The relatively small-scale variations, observed within even a single hole, generally cover the range of variability observed over larger scales (one hundred meters to over one kilometer) between Sites 921, 922, 923, and 924.

The dominant rock types which have been recovered at each of Sites 921, 922, 923, and 924 are gabbro and olivine gabbro. Troctolite, oxide gabbro, and leucocratic veins also occur in lesser volumes. Clinopyroxene in the gabbro is brown and occurs as a cumulus phase. In the olivine gabbro, clinopyroxene is either brown or green, and commonly occurs as oikocrysts. Olivine gabbro containing both brown cumulus clinopyroxene, and green poikilitic clinopyroxene has been recovered at Site 924, and may be transitional between the two dominant rock types. Olivine in the olivine gabbro and in the troctolite typically occurs as dark oikocrysts up to 60 mm in size. Where olivine is less abundant, it occurs as euhedral interstitial grains. Several recovered olivine gabbro intervals at Site 923 have dendritic and elongate olivine crystals that are associated with coarse, elongate, and in some places radiating, plagioclase laths. In thin section, these olivine crystals are optically continuous on the scale of 2 to 3 cm and are possible crescumulus morphologies. Another textural relationship commonly observed in olivine-rich rocks is one in which sparse, slender, and very elongate plagioclase laths are enclosed in the cores of clinopyroxene oikocrysts, but the plagioclase grain size outside of the core region of the oikocryst is 3 to 4 times that of the enclosed crystals. These and other textural features suggest that, within the crystallizing bodies where the drilled gabbroic rocks were formed, the relative nucleation and growth rates of plagioclase, clinopyroxene, and olivine may have varied substantially.

Primary magmatic layering occurs as changes in grain size, modal mineralogy, and rarely both across the same interface, on the scale of 1 cm up to a few meters. The attitude of this layering varies significantly within the cores, locally changing from subhorizontal to subvertical in a single long piece of core. Relatively high recovery at Site 923 provided significant insights into layering patterns that are only partially preserved in the other gabbro holes. In this hole, preliminary mesoscopic and thin-section observations suggest the occurrence of cycles of relatively primitive to somewhat more evolved rock types that may indicate recurrent evolutionary magmatic sequences. Each of these cycles is a few meters thick, and may record, to varying degrees, a transition from relatively primitive olivine gabbro, or troctolite, through olivine gabbro in which clinopyroxene occurs as an oikocryst phase, into olivine gabbro and gabbro with cumulus clinopyroxene (Fig. 10).

Oxide gabbro is a volumetrically minor but not uncommon lithology, particularly within Holes 921E, 922B, and 923A. It is found as irregular layers and stringers, mostly within the less olivine-rich lithologies, and is commonly associated with zones of high ductile shear strain. Plagioclase in oxide gabbro is commonly extensively recrystallized, and clinopyroxene forms blocky to elongate crystals. Orthopyroxene, zircon, and apatite are common associated phases.

Leucocratic veins up to a few centimeters thick also occur, particularly in rocks recovered from Sites 921 and 923. They commonly contain hornblende, apatite, and zircon. Quartz-bearing felsic veins have been observed in cores from Holes 921E and 923A. Primary minerals in these leucocratic veins are commonly pervasively altered. Actinolite and chlorite replace clinopyroxene, and secondary plagioclase, epidote, and prehnite commonly replace plagioclase.

These leucocratic veins, and the zircon and apatite-bearing oxide gabbro, are likely to represent crystallization products of evolved melts. Gabbroic rocks recovered at Sites 921 through 924 therefore appear to cover a wide range of compositions, from relatively primitive troctolite and olivine gabbro to lesser volumes of zircon and apatite-bearing gabbroic to trondhjemitic rocks.

Many gabbroic rocks recovered at Sites 921 to 924 contain essentially igneous textures including random-shape fabrics and weak foliations and/or lineations defined by the preferred shape orientation of strain-free elongate plagioclase, clinopyroxene, and/or olivine crystals. However, a remarkably wide range of crystal-plastic to cataclastic deformation fabrics are also developed. Crystal-plastic deformation is commonly concentrated in centimeter- to decimeter-scale shear zones in which primary minerals have undergone extreme grain-size reduction as a result of dynamic recrystallization. These shear zones commonly have downdip stretching lineations and display kinematic indicators suggesting normal displacements. The dip of these shear zones is variable, but most commonly exceeds 35°. Intervals of lineated gabbro with vertical dimensions of at least a few meters have also been observed at Sites 921 and 922. These contain intervals of olivine gabbro that are probably primary igneous layers, and irregular layers of highly deformed oxide gabbro.

Clinopyroxene is medium to coarse grained and weakly to moderately recrystallized, with elongate grains defining a mineral lineation. Plagioclase is moderately to intensely dynamically recrystallized.

Brittle deformation is limited to cataclastic zones and to several discrete generations of veins. Cataclastic shear zones occur in the upper sections of Holes 921B and 921C, and to a lesser extent in Hole 923A.These cataclastic shear zones are typically a few centimeters to decimeters thick and contain fractured, angular clasts of gabbroic material in a fine-grained cataclastic matrix. Evidence of crystal-plastic deformation within individual clasts suggests a complex interplay between brittle and crystal-plastic deformation mechanisms. The cataclastic shear zones have gently dipping orientations and are likely to be associated with the east-dipping fault surfaces seen in the surrounding outcrops.

Alteration of the igneous mineralogy is generally low (<10%) and very non-uniform at the decimeter to meter scale. Intervals of significantly more altered rocks (>90%) were recovered at Sites 922 and 924. In most of the gabbroic rocks from Sites 921 to 924, brown hornblende discontinuously rimming clinopyroxene, and as an interstitial phase, reflects the peak metamorphic temperatures. Some of this brown hornblende may have crystallized as a late igneous phase. Crystal-plastic shear zones commonly show evidence of syn-kinematic crystallization of brown hornblende, but the abundance of this hydrous phase is generally low. Hydrothermal alteration in most of the rocks recovered is dominated by static replacement of olivine by fine-grained oxide minerals, and a mesh of tremolite, actinolite, chlorite, smectite, talc, and trace amounts of carbonate minerals and pyrite. Alteration is slight in most samples, with more pervasive alteration typically limited to cataclastic zones, to the vicinity of crosscutting felsic veins, and to intervals with abundant hairline chlorite, chlorite and actinolite, and chlorite and smectite veins. In highly altered samples, clinopyroxene is overgrown by light green actinolite, and brown hornblende is partly replaced by olive green prismatic amphibole. Alteration coronas consisting of chlorite, tremolite-actinolite, and minor talc form at olivine/plagioclase grain boundaries. Plagioclase is replaced by chlorite, secondary plagioclase, prehnite, clay minerals, and minor epidote.

Gabbroic rocks cored at Sites 921 to 924 have complex remanent magnetizations, including components of both normal and reversed polarity. These multiple components suggest the possibility of intimately mixed intervals of different polarities. However, no systematic pattern of magnetization, with respect to either rock type or degree of alteration, is obvious from the presently available data. This complex magnetization history may preclude restoration of structural features in the cores to geographic coordinates, using paleomagnetic constraints. Reversed polarities, with values similar to the expected reversed-polarity dipole inclination (-41°), are dominant in rocks recovered at Sites 921 and 923. This suggests a minimum age of 0.7-0.9 Ma for these rocks. This inferred age is consistent with the age calculated for these rocks, using spreading rates deduced from regional magnetic anomaly studies (Schouten et al., 1987; Schulz et al., 1988). Remanence data from both the archive half-cores and discrete samples from Site 922, however, indicate predominantly normal magnetic polarity, with a mean inclination (42.2° + 3.6°, n = 15) also similar to the expected dipole inclination. High-stability components of dominantly shallow (0-30°), positive inclinations have also been determined at Site 924.

Despite the limited number of samples and the heterogeneous nature of the rocks recovered at Sites 921, 922, 923, and 924, variations in physical properties appear to correlate, at least in a general way, with the different rock types. Considering the entire data set, there appears to be no relationship between compressional wave velocity (V_p) and density for the different rock types recovered. This lack of correlation may be due to variations in mineral compositions, for example in iron/magnesium ratios. Bulk densities in the gabbroic rocks recovered at Sites 921 to 924 range from 2.76 to 3.03 g/cm^3, and porosities between 0.16% and 1.31%. Compressional wave velocity measured at 1 atm ranges between 4.7 and 6.6 km/s. Densities, velocities, and porosities determined at Site 923 are comparable to those measured in gabbroic rocks recovered during previous hard-rock legs (Legs 118 and 147). Velocities measured in samples from the other sites are up to 1 km/s slower, but similar to those measured in dredged gabbroic samples from fracture zones in the Atlantic (Christensen, 1982). Thermal conductivities of between 2.3 and 3.0 W/m°C in rocks from Sites 921, 922, 923, and 924 are slightly higher than those measured in Leg 118 and Leg 147 gabbroic rocks, but are still within the range of values characteristic of gabbroic rocks.

CONCLUSIONS

Investigations over the past 30 years have made the MARK area the most extensively studied portion of any slow-spreading ridge. Extensive geological and geophysical surveys have permitted a detailed picture of the composition and structure to be constructed that is far beyond that possible elsewhere. These data have permitted the development of new and sometimes provocative models for seafloor spreading that could not have been inferred from less comprehensive data. A significant part of these investigations has been directly related to ODP site surveys and drilling. Furthermore, ODP drilling clearly is required to test many important hypotheses for the creation and evolution of oceanic crust in the slow-spreading environment present in the MARK area (e.g. Dick et al., 1981; Pockalny et al., 1988; Karson, 1991; Karson and Winters, 1992; Sinton and Detrick, 1992; Cannat, 1993).

While drilling the hard-rock foundation of the ocean floor has proven to be a daunting engineering challenge, following success in drilling plutonic rocks exposed where the oceanic crust had been stripped of its basaltic carapace on Legs 109 and 118, a strategy for drilling a series of relatively shallow, closely spaced holes that could be correlated laterally (offset drilling) was proposed. Leg 153 represents the second ODP offset drilling leg, in this case devoted to drilling the plutonic foundation of slow-spreading (~25 mm/yr) oceanic lithosphere in the MARK area. Exposures of coarse-grained mafic and ultramafic rocks on the median-valley walls are considered to be <1 Ma and to have resulted from mechanical extension of the axial lithosphere during a period of limited magmatic construction. The sites drilled during Leg 153 are located in the footwalls of major detachment faults cutting ultramafic and gabbroic rocks, respectively. For Leg 153, the ODP returned to the MARK area armed with an impressive array of new tools and techniques that had been developed over the course of several legs of hard-rock drilling. With these new approaches, it was hoped that significant progress could be made in drilling the major rock units exposed in the area and that new insights into slow-spreading ridges could be gained.

Most of the material recovered from Site 920 is serpentinized harzburgite. Despite the intense alteration of the rock to serpentine, typically greater than 80%, primary mineralogy and textures can be inferred from distinctive pseudomorphs and local patches of relatively fresh material. Locally the serpentinized harzburgite contains interlayered pyroxene-rich (up to 35% orthopyroxene) and pyroxene-poor harzburgite to dunite. Of special interest are numerous elongated segregations or veins of spinel, clinopyroxene, plagioclase, or a combination of these phases that are interpreted as material that crystallized along former melt channels in the peridotite. Pegmatitic gabbroic intervals a few centimeters to a few tens of centimeters thick are also intercalated within the serpentinized harzburgite. Deformation features bear witness to a complex strain history over progressively decreasing temperatures. These early, high-temperature features are overprinted in most samples by an anastomosing foliation, highlighted by thin, white serpentine veins. This foliation appears to result from the preferred orientation of fine, discontinuous veins of serpentine, and serpentine and iron oxide minerals cutting the background serpentine network. The anastomosing serpentine fabric is cut by later generations of serpentine-bearing extensional and sheared veins. The relative intensity and dip of the high-temperature pyroxene foliation, anastomosing serpentine foliation, and the densities of discrete vein arrays vary considerably along the lengths of the cores. These characteristics integrate in various ways to define several distinct structural domains. Several distinctive mafic and ultramafic units have been tentatively correlated between the two holes. The serpentinized harzburgite has very high natural remanence and susceptibility. The measured inclination is similar to the present field for this location, and therefore the orientations of various structures in the core may be at least partially corrected. Preliminary physical-properties results show good correlations with the rock types and degree of alteration.

The gabbroic rocks recovered from Sites 921, 922, 923, and 924 display large variations in composition, grain size, texture, degree of deformation, and extent of alteration. The textural variations, commonly occurring over length scales of a few centimeters to tens of centimeters, suggest crystallization in an environment characterized by high thermal gradients and syn- to post-magmatic deformation. Generally, the rocks include meter-scale layers of gabbro and olivine gabbro, with lesser troctolite and iron-titanium oxide gabbro. Meter-scale diabase dikes with chilled margins are also present. Alteration of the igneous mineralogy is generally low and very non-uniform at the decimeter to meter scale. Rare, highly altered sections throughout the core are typically restricted to narrow mylonite and cataclastic zones, and to the vicinity of crosscutting felsic veins. Plagioclase in the gabbroic rocks has commonly experienced crystal-plastic deformation, resulting in a weak shape fabric defined by elongated mafic phases. Trondhjemitic veins, 20-30 mm wide, are sparsely distributed throughout the cores. Primary minerals in these veins are commonly pervasively replaced. Gabbroic rocks cored at Sites 921-924 have complex remanent magnetizations, including components of both normal and reversed polarity. However, no systematic pattern of magnetization, with respect to either rock type or degree of alteration, is obvious from the presently available data. Variations in physical-properties measurements appear to correlate with the different rock types. Densities, velocities, and porosities determined at Site 923 are comparable to those measured in gabbroic rocks recovered during previous hard-rock legs (Legs 118 and 147). Velocities measured in samples from the other sites are slower, but similar to those measured in dredged gabbroic samples. Thermal conductivities measured on samples from Sites 921, 922, 923, and 924 are within the range of values characteristic of gabbroic rocks.

Although the MARK area is the most extensively studied part of the Mid-Atlantic Ridge, direct observations of subsurface characteristics are lacking. Nearly all of the samples from the region collected to date have been dredged or collected by submersible, providing limited information on spatial or temporal relationships and the geometry of structural features. Additionally, all samples collected from the surface suffer from a low-temperature overprint on any high-temperature deformation or alteration characteristics. Drilling provides the only method whereby subcontinuous sampling allows definition of the nature and orientation of igneous, metamorphic, and structural contacts, and penetrates through the veil of low-temperature alteration effects common to other sampling techniques. Recent studies of the Mid-Atlantic Ridge demonstrate that the interplay of magmatic construction and mechanical extension varies significantly both regionally and even locally. Still, information derived from studies of plutonic rocks and major fault zones drilled in the northern spreading cell of the MARK area should be widely applicable to other segments of slow-spreading ridges.

REFERENCES

Auzende, J.M., Cannat, M., Gente, P., Henriet, J.P., Juteau, T., Karson, J.A., Lagabrielle, Y., and Tivey, M.A., 1993. A transect through 0-4 Ma oceanic crust: *Nautile* dives along the Kane Transform. *RIDGE Events*, 4:3-10.

Brown, J.R., and Karson, J.A., 1988. Variations in axial processes on the Mid-Atlantic Ridge: the median valley of the MARK area. *Mar. Geophys. Res.,* 10:109-138.

Bryan, W.F., Humphris, S., Thompson, G., and Casey, J.F., in press. Comparative volcanology of small eruptive centers in the MARK area. *J. Geophys. Res.*

Bryan, W.B., Thompson, G., and Ludden, J.N., 1981. Compositional variation in normal MORB from 22-25°N: Mid-Atlantic Ridge and Kane Fracture Zone. *J. Geophys. Res.*, 86:11815-11836.

Cannat, M., 1993. Emplacement of mantle rocks in the seafloor at mid-ocean ridges. *J. Geophys. Res.*, 98:4163-4172.

Cannat, M., Mévél, C., Maia, M., Durand, C., Gente, P., Deplus, C., Agrinier, P., Belarouchi, A., Dubuisson, G., Humler, E., and Reynolds, J., 1993. Crustal structure and axial segmentation, Mid-Atlantic Ridge 21-24°N. *Eos*, 74:664.

Christensen, N.I., 1992. Seismic velocities. *In* Carmichael, R.S. (Ed.), *Handbook of physical properties of rocks, Volume II*: Boca Raton, Florida (CRC Press, Inc.), 1-229.

Cormier, M., Detrick, R.S., and Purdy, G.M., 1984. Anomalously thin crust in oceanic fracture zones, new seismic constraints from the Kane fracture zone. *J. Geophys. Res.,* 89:10249-10266.

Delaney, J.R., Mogk, D.W., and Mottl, M.J., 1985. Quartz-cemented, sulfide-bearing greenstone breccias from the Mid-Atlantic Ridge - samples of a high temperature hydrothermal upflow zone. *J. Geophys. Res.*, 92:9175-9192.

Deplus, C., Maia, M., Aslanian, D., and Gente, P., 1992. Segmentation of the Mid-Atlantic Ridge south of Kane fracture zone revealed by gravity anomalies. Results of *Seadma 1* cruise. *Eos,* 73:568.

Detrick, R.S., Fox, P.J., Kastens, K., Ryan, W.B.F., Mayer, L., and Karson, J., 1984. A Sea Beam survey of the Kane fracture zone and adjacent Mid-Atlantic rift valley. *Eos*, 65:1006.

Detrick, R.S., Fox, P.J., Schulz, N., Pockalny, R., Kong, L., Mayer, L., and Ryan, W.B.F., 1988. Geologic and tectonic setting of the MARK area. *In* Detrick, R., Honnorez, J., Bryan, W.B., Juteau, T., et al., *Proc. ODP, Init. Repts. (Pt. A)*, 106/109:College Station, TX (Ocean Drilling Program), 15-22.

Detrick, R.S., Mutter, J.C., Buhl, P., and Kim, I.I., 1990. No evidence from multichannel seismic reflection data for a crustal magma chamber in the MARK area on the Mid-Atlantic Ridge. *Nature*, 347:61-64.

Detrick, R.S., and Purdy, G.M., 1980. Crustal structure of the Kane Fracture Zone from seismic refraction studies. *J. Geophys. Res.*, 85:3759-3777.

Dick, H.J.B., Thompson, G., and Bryan, W.B., 1981. Low angle faulting and steady state emplacement of plutonic rocks at ridge-transform intersections. *Eos*, 62:406.

Fox, P.J., 1972. The geology of some Atlantic fracture zones, Caribbean escarpments, and the nature of the oceanic basement and crust [Ph.D. dissert.]. Columbia University, New York.

Gente, P., Aslanian, D., Campan, A., Cannat, M., Ceuleneer, G., Deplus, C., Durand, C., Laverne, C., Leau, H., Maia, M., Marion, E., Mével, C., Pockalny, R., and Seyler, M., 1991. Geometry of past and present day segmentation of the Mid-Atlantic Ridge, south of Kane fracture zone. *Eos,* 72:477.

Gente, P., Zonenshain, L.P., Kuzmin, M., Lisitsin, A.P., Bogdanov, Y.A., and Baronov, B.V., 1989. Géologie de l'axe de la dorsale médio-Atlantique entre 23 et 26°N: résultats préliminaires de la 15ème campagne du N/O Akademik Mstyslav Keldysh (mars-avril 1988). *C.R. Acad. Sci.,* 308:1781-1788.

Gillis, K.M., Thompson, G., and Kelley, D.S., 1993. A view of the lower crustal component of hydrothermal systems at the Mid-Atlantic Ridge. *J. Geophys. Res.*, 98:19597-19620.

Juteau, T., Berger, E., and Cannat, M., 1990. Serpentinized, residual mantle peridotites from the MAR median valley, ODP Hole 670A (21°10'N, 45°2'W, Leg 109): Primary mineralogy and geothermometry. *In* Detrick, R., Honnorez, J., Bryan, W.B., Juteau, T., et al., *Proc. ODP, Sci. Results*, 106/109: College Station, TX (Ocean Drilling Program), 27-45.

Karson, J.A., 1991. Seafloor spreading on the Mid-Atlantic Ridge: Implications for the structure of ophiolites and oceanic lithosphere produced in slow-spreading environments. *In* Malpas, J., Moores, E.M., Panayiotou, A., and Xenophontos, C. (Eds.), Proceedings of the Symposium "Troodos 1987": Geological Survey Department Nicosia, Cyprus, 547-555.

Karson, J.A., Delaney, J.R., Spiess, F.N., Hurst, S., Lawhead, B., Bigger, S., Naidoo, D., and Gente, P., 1992a. Deep-tow observations at the eastern intersection of the Mid-Atlantic Ridge and the Kane Fracture Zone. *Eos*, 73:552.

Karson, J.A., Delaney, J.R., and Spiess, F.N., 1992b. Vertically layered mafic-ultramafic complex observed on the seafloor. *RIDGE Events*, 3:3-4.

Karson, J.A., and Dick, H.J.B., 1983. Tectonics of ridge-transform intersections at the Kane fracture zone. *Mar. Geophys. Res.*, 6:51-98.

Karson, J.A., Thompson, D.G., Humphris, S.E., Edmond, J.M., Bryan, W.B., Brown, J.R., Winters, A.T., Pockalny, R.A., Casey, J.F., Campbell, A.C., Klinkhammer, G., Palmer, M.R., Kinzler, R.J., and Sulanowska, M.M., 1987. Along axis variation in seafloor spreading in the MARK area. *Nature,* 328:681-685.

Karson, J.A., and Winters, A.T., 1992. Along-axis variations in tectonic extension and accommodation zones in the MARK area, Mid-Atlantic Ridge 23°N. *In* Parsons, L.M., Murton, B.J., and Browning, P. (Eds.), *Ophiolites and their modern oceanic analogues*. Geol. Soc. Spec. Publ. London, 60:107-116.

Kelley, D.S., and Delaney, J.R., 1987. Two phase separation and fracturing in mid-oceanic ridge gabbros at temperature greater than 700°C. *Earth Planet. Sci. Lett.,* 83:53-66.

Kelley, D.S., Gillis, K.M., and Thompson, G., 1993. Fluid evolution in submarine magma-hydrothermal systems at the Mid-Atlantic Ridge. *J. Geophys. Res.,* 98:19579-19598.

Komor, S.C., Grove, T.L., and Hébert, R., 1990. Abyssal peridotites from ODP Hole 670A (21°10'N, 45°02'W): Residues of mantle melting exposed by non-constructive axial divergence. *In* Detrick, R., Honnorez, J., Bryan, W.B., Juteau, T., et al., *Proc. ODP, Sci. Results*, 106/109: College Station, TX (Ocean Drilling Program), 85-102.

Kong, L.S.L., Detrick, R.S., Fox, P.J., Mayer, L.A., and Ryan, W.F.B., 1988. The morphology and tectonics of the MARK area from Sea Beam and MARC 1 observations (Mid-Atlantic Ridge 23°N). *Mar. Geophys. Res.*, 10:59-90.

Kuo, B.-Y., and Forsyth, D.W., 1988. Gravity anomalies of the ridge transform system in the South Atlantic between 31° and 34°S. *Mar. Geophys. Res.*, 10:205-232.

Lin, J., Purdy, G.M., Schouten, H., Sempere, J.C., and Zervas, C., 1990. Evidence from gravity data for focused magmatic accretion along the Mid-Atlantic Ridge. *Nature*, 344:627-632.

Louden, K.E., and Forsyth, D., 1982. Crustal structure and isostatic compensation near the Kane Fracture Zone from topography and gravity measurements - I spectral analysis approach. *Geophys. J. R. Astron. Soc.*, 68:38-52.

Marion, E., 1993. Interactions croute oceanique profonds-eau de mer dans les gabbros de la zone MARK (Mid-Atlantic Ridge/Kane Fracture Zone) [Ph.D. thesis]. Université Pierre et Marie Curie, Paris.

Marion, E., Mével, C., and Cannat, M., 1991. Evolution of oceanic gabbros from the MARK/Kane fracture intersection massif. *TERRA Abstracts*, 3:310.

Melson, W.G., Thompson, W.G., and van Andel, T.H., 1968. Volcanism and metamorphism in the Mid-Atlantic Ridge, 22°N. *J. Geophys. Res.*, 73:5925-5941.

Mével, C., Cannat, M., Gente, P., Marion, E., Auzende, J.M., and Karson, J.A., 1991. Emplacement of deep crustal and mantle rocks on the West median valley wall of the MARK area (M.A.R. 23°N). *Tectonophysics*, 190:31-53.

Miyashiro, A., Shido, F., and Ewing, M., 1969. Composition and origin of serpentinites from the Mid-Atlantic Ridge, 24° and 30°N. *Contrib. Mineral. Petrol.*, 32:38-52.

Miyashiro, A., Shido, F., and Ewing, M., 1970. Petrologic models for the Mid-Atlantic Ridge. *Deep-Sea Res.,* 17:109-125.

Miyashiro, A., Shido, F., and Ewing, M., 1971. Metamorphism in the Mid-Atlantic Ridge near 24° and 30°N. *Phil. Trans. Roy. Soc. London,* A268:589-603.

Morris, E., and Detrick, R.S., 1991. Three dimensional analysis of gravity anomalies in the MARK area (MAR, 23°N). *J. Geophys. Res.,* 96:4355-4366.

Mutter, J.C., and Karson, J.A. , 1992. Structural processes at slow-spreading ridges. *Science,* 257:627-634.

ODP Leg 106 Scientific Party, 1986. Drilling the Snake Pit hydrothermal deposit on the Mid-Atlantic Ridge. *Geology*, 14:1004-1007.

Patriat, P., Deplus, C., Rommevaux, C., and Sloan, H., 1991. SARA: Evolution of the axial segmentation of the Mid Atlantic Ridge between 28° and 29°N, 0-10 Ma. *Eos*, 72:477.

Pockalny, R.A., Detrick, R.S., and Fox, P.J., 1988. Morphology and tectonics of the Kane transform from Sea Beam bathymetry data. *J. Geophys. Res.*, 93:3179-3193.

Purdy, G.M., and Detrick, R.S., 1986. Crustal Structure of the Mid-Atlantic ridge at 23°N from seismic refraction studies. *J. Geophys. Res.*, 91:3739-3762.

Purdy, G.M., Rabinowitz, P.D., and Schouten, H., 1979. The Mid-Atlantic Ridge at 23°N: Bathymetry and magnetics. *In* Melson, W.G., Rabinowitz, P.D., et al., *Init. Repts. DSDP*, 45: Washington (U.S. Govt. Printing Office), 119-128.

Schouten, H., Dick, H.J.B., and Klitgord, K.D., 1987. Migration of mid-oceanic ridge segments. *Nature,* 326:835-839.

Schulz, N.J., Detrick, R.S., and Miller, S.P., 1988. Two and three-dimensional inversions of magnetic anomalies in the MARK area (Mid-Atlantic Ridge, 23°N). *Mar. Geophys. Res.*, 10:41-57.

Searle, R., Lawson, K., Pearce, J., Allerton, S., Browning, P., Kempton, P., Mével, C., Murton, B., and Schouten, H., 1992. Volcanic and tectonic development of the Mid-Atlantic Ridge north of the Kane Transform: MARNOK, 24°-25°N. *Eos,* 73:569.

Sinton, J.M., and Detrick, R.S., 1992. Mid-ocean ridge magma chambers. *J. Geophys. Res.*, 97:197-216.

Toomey, D.R., Solomon, S.C., and Purdy, G.M., 1988. Microearthquakes beneath the median valley of the Mid-Atlantic Ridge near 23°N; tomography and tectonics. *J. Geophys. Res.*, 93:9093-9112.

Toomey, D.R., Solomon, S.C., Purdy, G.M., and Murray, M.H., 1985. Microearthquakes beneath the median valley of the Mid-Atlantic Ridge near 23°N; hypocenters and focal mechanism. *J. Geophys. Res.,* 90:5443-5458.

van Andel, T.H., Phillips, J.D., and Von Herzen, R.P., 1969. Rifting origin for the Vema fracture zone in the North Atlantic. *Earth Planet. Sci. Lett.*, 5:296-300.

Table 1

Geological and Geophysical Investigations in the MARK Area

Study	Technique	Area	References
Bathymetry	Single Channel Echo-Sounder	22°-24°N on the MAR	Purdy et al., 1979
	Sea Beam	MAR Axis 22°-24°N and Kane F.Z.	Kong et al., 1988
	Sea Beam	MAR Axis 24°-22°30'N (gaps)	Karson et al., 1987
	Simrad	MAR and seafloor to 10 Ma 24°-20°N	Gente et al., 1991
Magnetics	Surface Ship	MAR and seafloor to 10 Ma 24°-20°N	Gente et al., 1991
	Surface Ship	MAR Axis 22°-24°N and Kane F.Z.	Schulz et al., 1988
Gravity	Surface Ship	Kane Transform	Louden and Forsyth, 1982
	Surface Ship	MAR Axis 22°-24°N and Kane F.Z.	Morris and Detrick, 1991
	Surface Ship	MAR and Crust to 10 Ma 24°-20°N	Deplus et al., 1992
	Near-Bottom (from *Nautile*)	MAR Axis at 23°20'N	Dubois et al., unpub. data
Seismics	Refraction	Kane F.Z.	Detrick and Purdy, 1980
	Refraction	MAR Axis 22°-24°N (Kane F.Z.)	Purdy and Detrick, 1986
	Delay-Time Studies	Nodal Basin at E RTI of Kane F.Z.	Cormier et al., 1984
	MCS Reflection	MAR Median Valley 22°30'-24°N	Detrick et al., 1990; Mutter and Karson, 1992
	Microseismic Network	MAR Median Valley at 22°40'N	Toomey et al., 1985, 1988
Side-Scan Sonar	Sea MARC I	MAR Axis 22°15'-23°30'N	Kong et al., 1988
	TOBIE	W. Kane Transform and W RTI	Searle et al., 1992
	Deep Tow: Up/Down-Looking Sonar	E. Kane Transform and E RTI	Karson et al., 1992a
Near-Bottom Photogeology	ANGUS	Kane F.Z. and MAR at E and W RTI's	Karson and Dick, 1983
	ANGUS	MAR 22°50'-23°N	Karson et al., 1987; Brown and Karson, 1988
	Deep Tow	E. Kane F.Z. and MAR at E RTI	Karson et al., 1992b
	SCAMPI	MAR 22°-22°30'N	Cannat et al., unpub. data
Submersible Dives	*Alvin*	W. Wall, E RTI	Karson and Dick, 1983
	Alvin	MAR Median Valley 23°15'-22°55'N	Karson et al., 1987; Brown and Karson, 1988
	Nautile	MAR Median Valley 23°40'-23°15'N	Mével et al., 1991; Gente et al., 1991
	Nautile	Kane F.Z. at E RTI	Auzende et al., 1993
	Nautile	MAR Median Valley 23°40'-23°15'N	Dubois et al.,unpub. data

Table 1 cont.

Study	Technique	Area	References
Ocean Drilling Program	*JOIDES Resolution*, Leg 106	MAR Axis at 23°15'N (Snake Pit Vent Site)	Detrick et al., 1988; Proc. ODP, Leg 106
	JOIDES Resolution, Leg 109	MAR Axis at 22°55'N and 23°15'N	Detrick et al., 1988; Proc. ODP, Leg 109
	JOIDES Resolution, Leg 153	MAR Median Valley Wall at 23°31'N and 23°05'N	unpub. data
Dredging	Dredging	MAR Median Valley at 22°-23°N	Melson et al., 1968
	Dredging	Kane Transform	Miyashiro et al., 1969, 1971
	Dredging	MAR Median Valley at 22°-24°N	Bryan et al., 1981
	Dredging and *Alvin*	MAR at 24°N	Karson and Dick, 1983
	Dredging and *Alvin*	MAR Median Valley at 22°-24°N	Karson et al., 1987; Bryan et al., in press.
	Dredging	MAR Median Valley at 22°-24°N	Zonenshain et al., unpub. data; Gente et al., 1989
	Dredging	MAR and seafloor to 4 Ma, 21°-24°N	Cannat et al., 1993

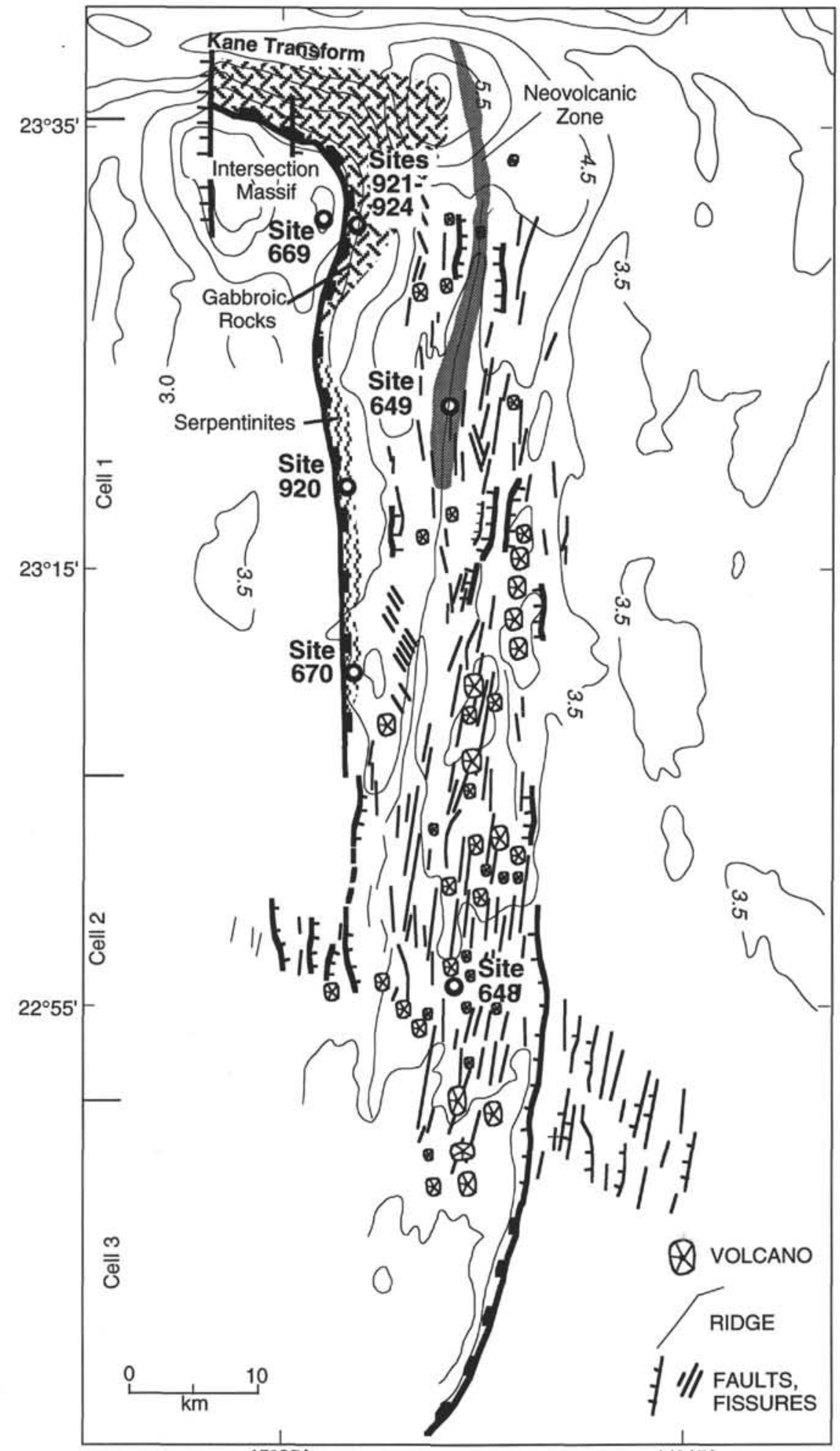

Figure 1. General bathymetric map of the MARK area. Recent ODP sites shown as open circles. Perpendicular hachures represent area of outcrop of gabbroic rocks, zig-zag line represents area of serpentinite outcrops, identified from submersible studies and dredging. Discrete spreading segments, or cells, described in text. Contours in km below sea level.

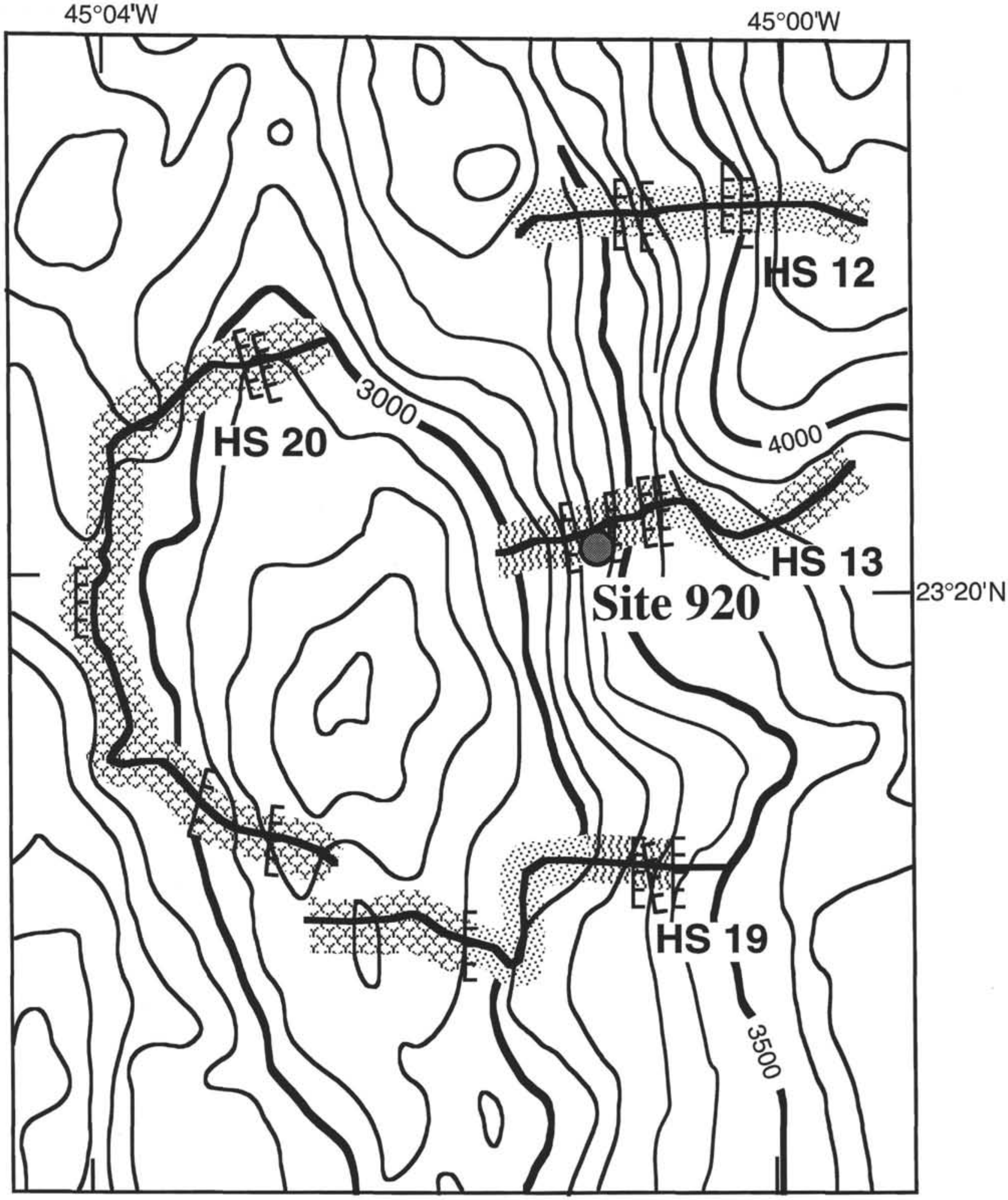

Figure 2. Bathymetric map of area near Site 920. Contour values in meters. Lithologies recorded by *Nautile* (HS, Mével et al., 1991) dives (tracks shown in bold, solid lines crossing contours). Zig-zag lines=peridotite outcrops; y's=basalt outcrops; stipple=rubble and sediment. Hachured lines represent faults; hachures on downthrown side.

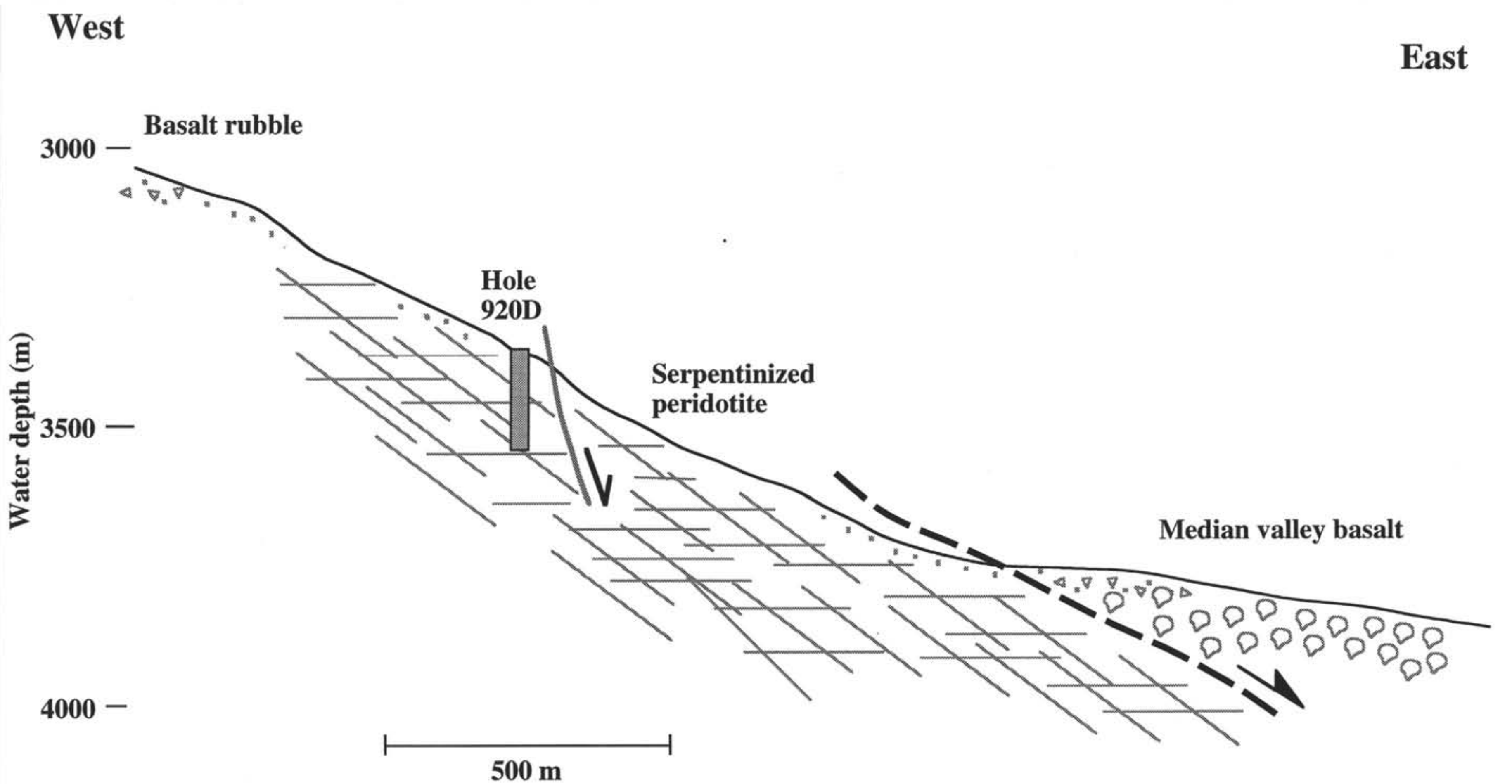

Figure 3. Schematic cross section of the western median valley wall at 23°20.32'N, from *Nautile* dive HS 13 and Site 920 camnera survey. No vertical exaggeration.

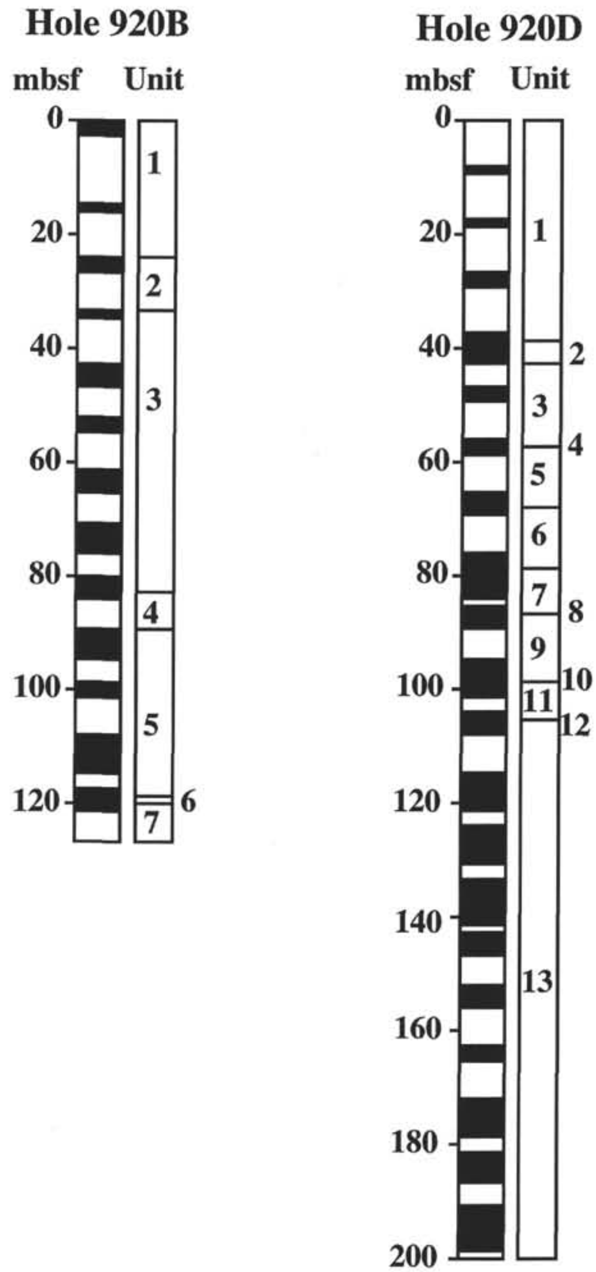

Figure 4. Schematic recovery and lithologic units for Holes 920B and 920D.

Lithologic units for Hole 920B:

1- Serpentinized harzburgite; 2- Pyroxene-rich serpentinized harzburgite; 3- Serpentinized harzburgite; 4- Diabase; 5- Serpentinized harzburgite; 6- Oxide-rich metagabbro; 7- Amphibolite and gneissic gabbro.

Lithologic units for Hole 920D:

1- Serpentinized harzburgite; 2- Pyroxene-rich serpentinized harzburgite; 3- Serpentinized harzburgite; 4- Amphibolitized microgabbro; 5- Serpentinized harzburgite; 6- Diabase; 7- Serpentinized harzburgite; 8- Rodingitized gabbro; 9- Serpentinized harzburgite; 10- Pegmatitic oxide-rich gabbro; 11- Serpentinized harzburgite; 12- Oxide-rich metagabbro; 13- Serpentinized harzburgite.

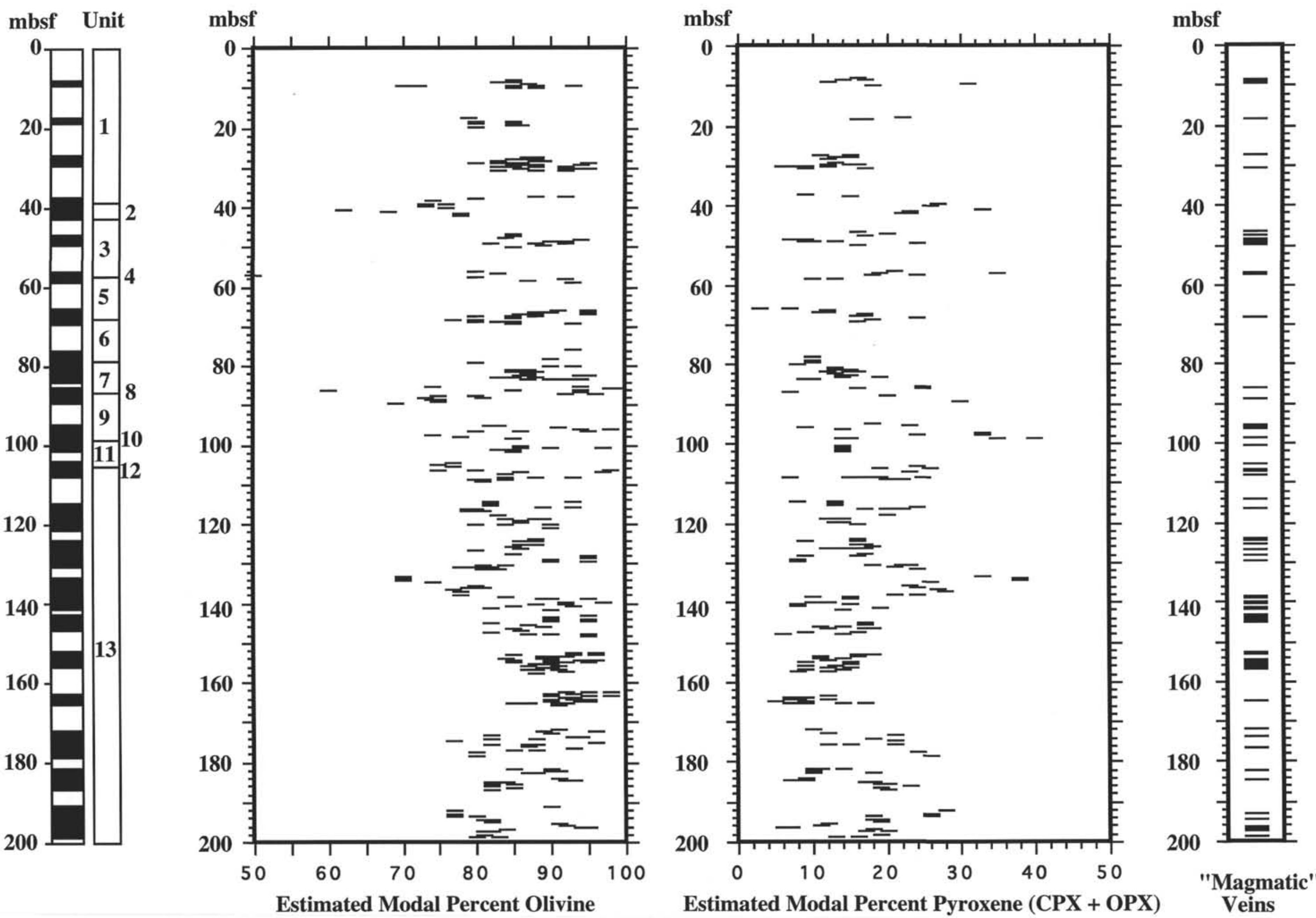

Figure 5. Variation of modal olivine and pyroxene with depth in Hole 920D. Column on right indicates magmatic vein or dike occurrences (each line represents the occurrence of a vein or dike which may be a few millimeters to a few centimeteres across).

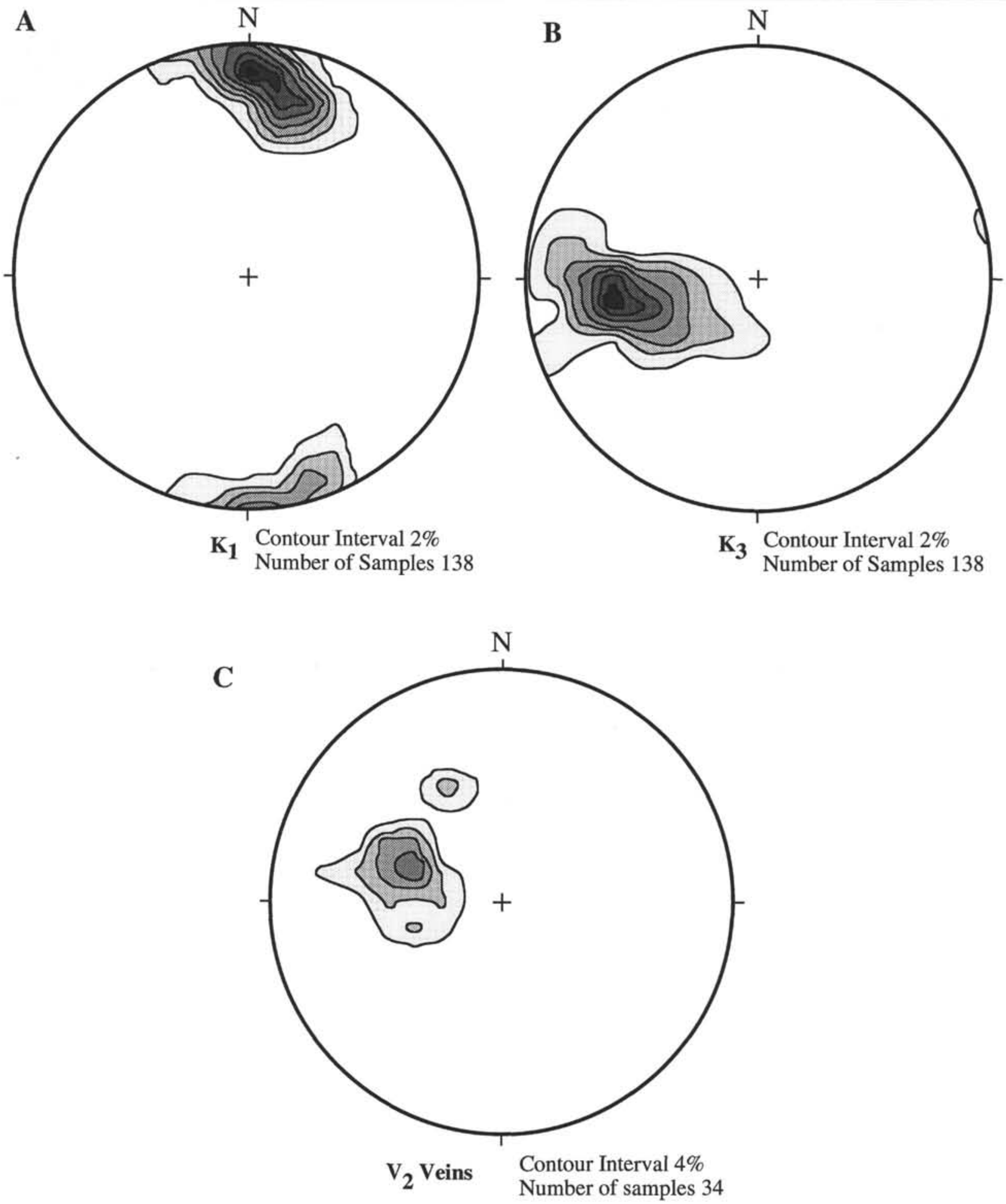

Figure 6. Lower hemisphere contour plots of magnetic fabric and vein orientation data (poles to V_2 vein set) after azimuthal reorientation of characteristic remanent declination to 360°. The maximum (K_1) and minimum (K_3) axes of the susceptibility ellipsoid are directed approximately north and west, respectively. The magnetic "foliation" is approximately parallel to the anastomosing fabric defined by V_2 veins and coplanar pyroxene foliation. Note that the strong maxima are the result of cores having been cut normal to the anastomosing foliation.

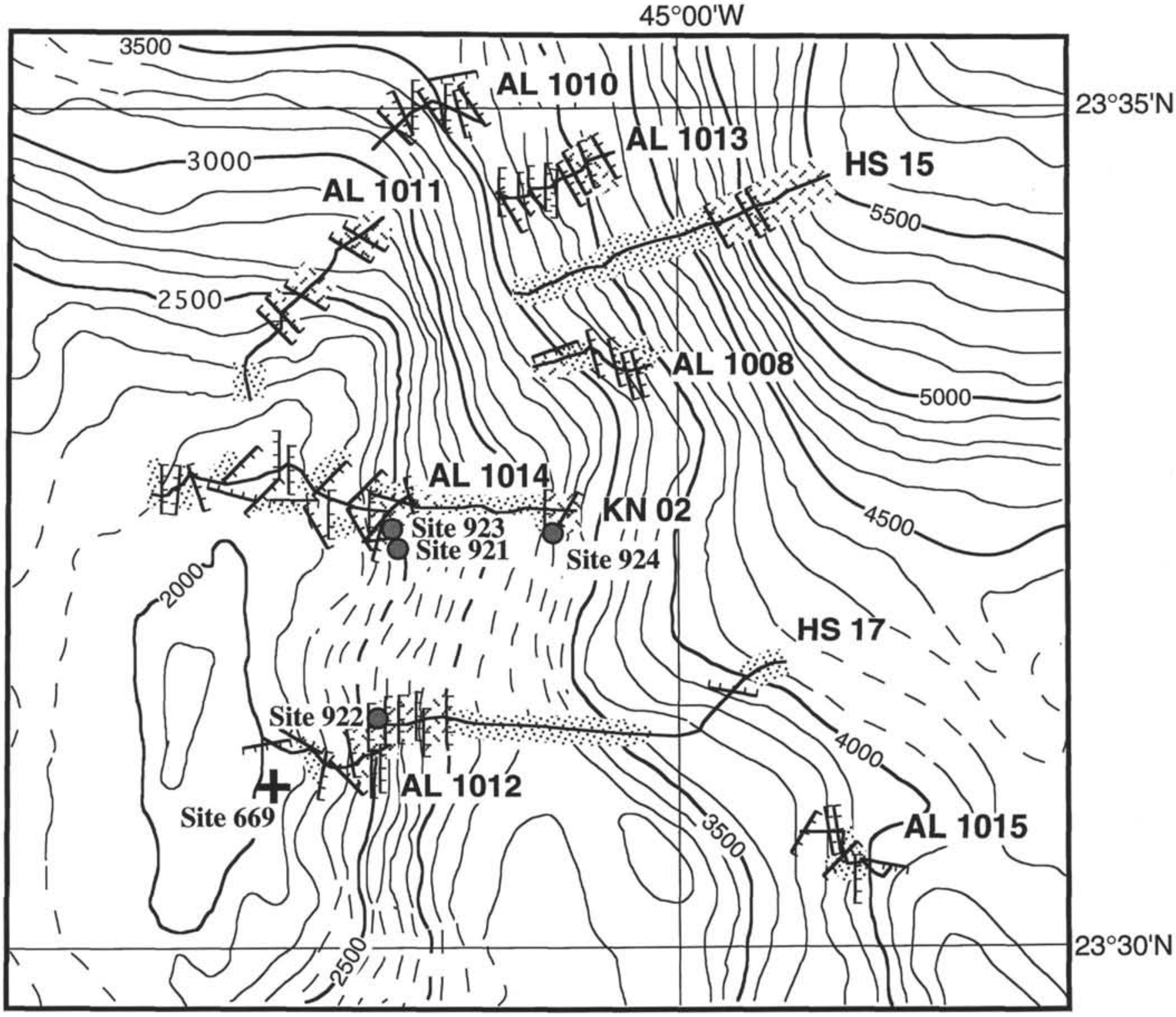

Figure 7. Bathymetric map (in meters) of the western wall of the MAR in the MARK area about 5 km south of the Kane Transform. Dive tracks of *Alvin* (Al 1008, Al 1010-1014) and *Nautile* (HS 15, 17, and KN 02) show numerous east-facing escarpments and extensive exposures of variably deformed and metamorphosed gabbroic rocks (random dashed pattern) and rubble derived from these exposures (stippled pattern). Sites 921-923 are located at about 2500 m water depth among a series of cliffs of gabbroic rock.

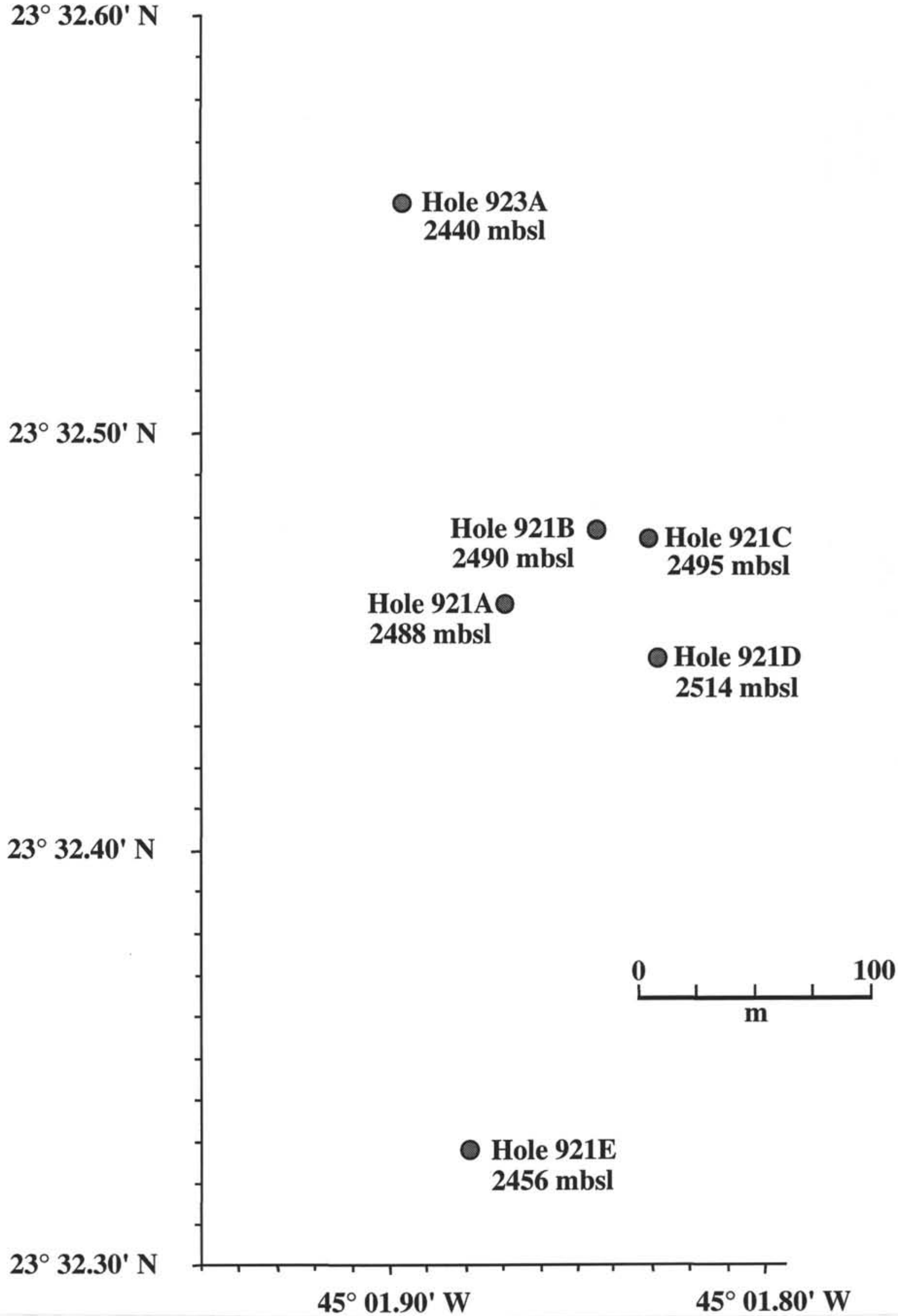

Figure 8. Positions of Holes 921A-E and 923A. Holes 923A and 921E are offset ~150 m north and 200 m south, respectively, from the series of Holes 921A-D.

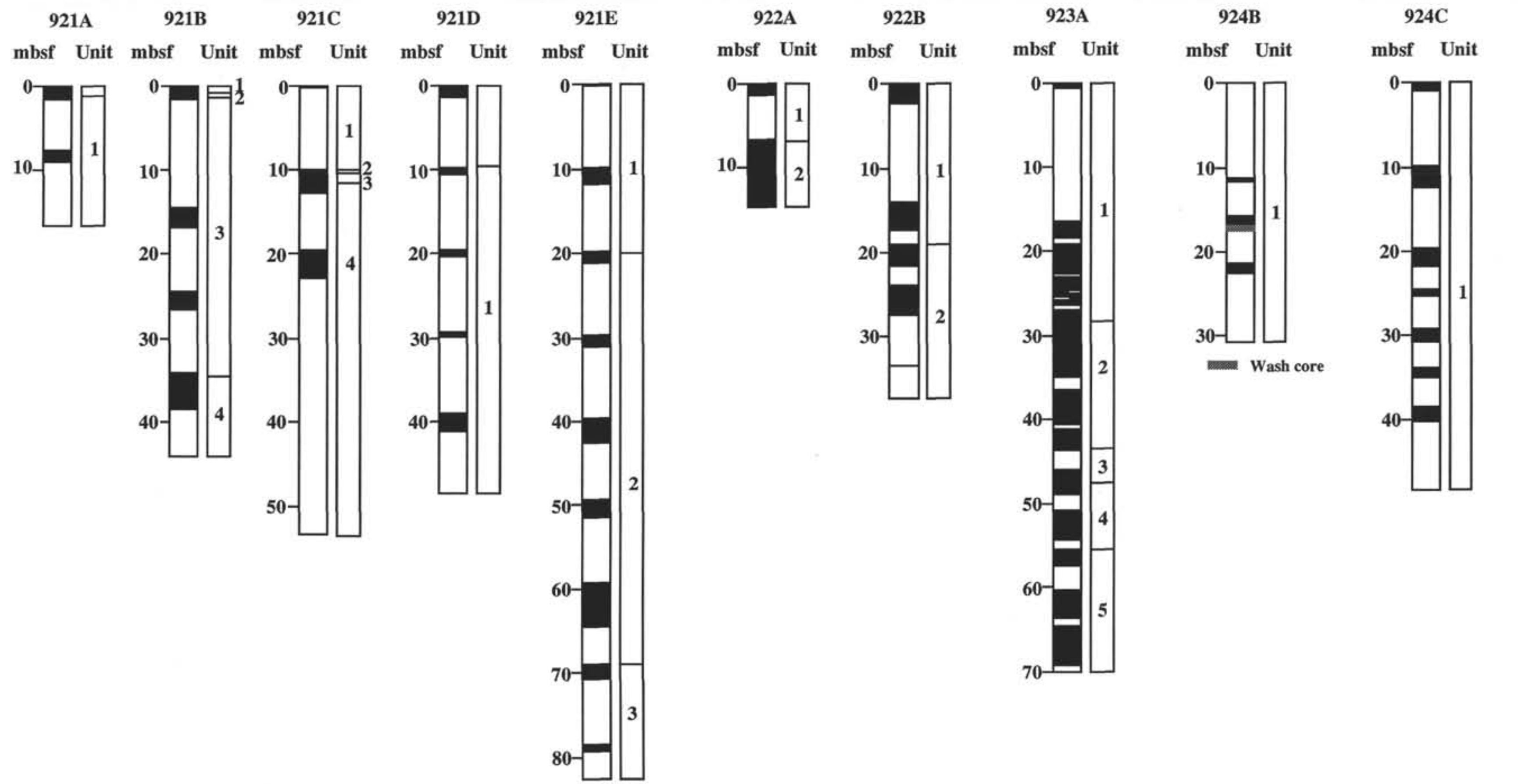

Figure 9. Schematic recovery and lithologic unit columns for all holes from Sites 921-924.

Lithologic units for Hole 921A: 1- Olivine gabbro.

Lithologic units for Hole 921B:
1- Cataclastic metagabbro;
2- Aphyric to sparsely phyric diabase;
3- Lineated gabbro;
4- Poikilitic olivine gabbro.

Lithologic units for Hole 921C:
1- Cataclastic metagabbro;
2- Aphyric to sparsely phyric diabase;
3- Lineated gabbro;
4- Poikilitic olivine gabbro.

Lithologic units for Hole 921D: Mixed gabbro/olivine gabbro.

Lithologic units for Hole 921E: 1- Very coarse-grained to pegmatitic gabbro;
2- Heterogeneous poikilitic olivine gabbro; 3- Vari-textured gabbro/olivine gabbro.

Lithologic units for Hole 922A:
1- Metatroctolite;
2- Troctolite and olivine gabbro.

Lithologic units for Hole 922B:
1- Troctolite and olivine gabbro;
2- Poikilitic olivine gabbro.

Lithologic units for Hole 923A:
1- Variably deformed gabbro and olivine gabbro; 2- Interlayered troctolite and olivine gabbro; 3- Poikilitic olivine gabbro and troctolite; 4- Vari-textured gabbro and olivine gabbro;
5- Troctolite and poikilitic olivine gabbro.

Lithologic units for Hole 924B: 1- Lineated gabbro/olivine gabbro.

Lithologic units for Hole 924C:
1- Poikilitic olivine gabbro/troctolite.

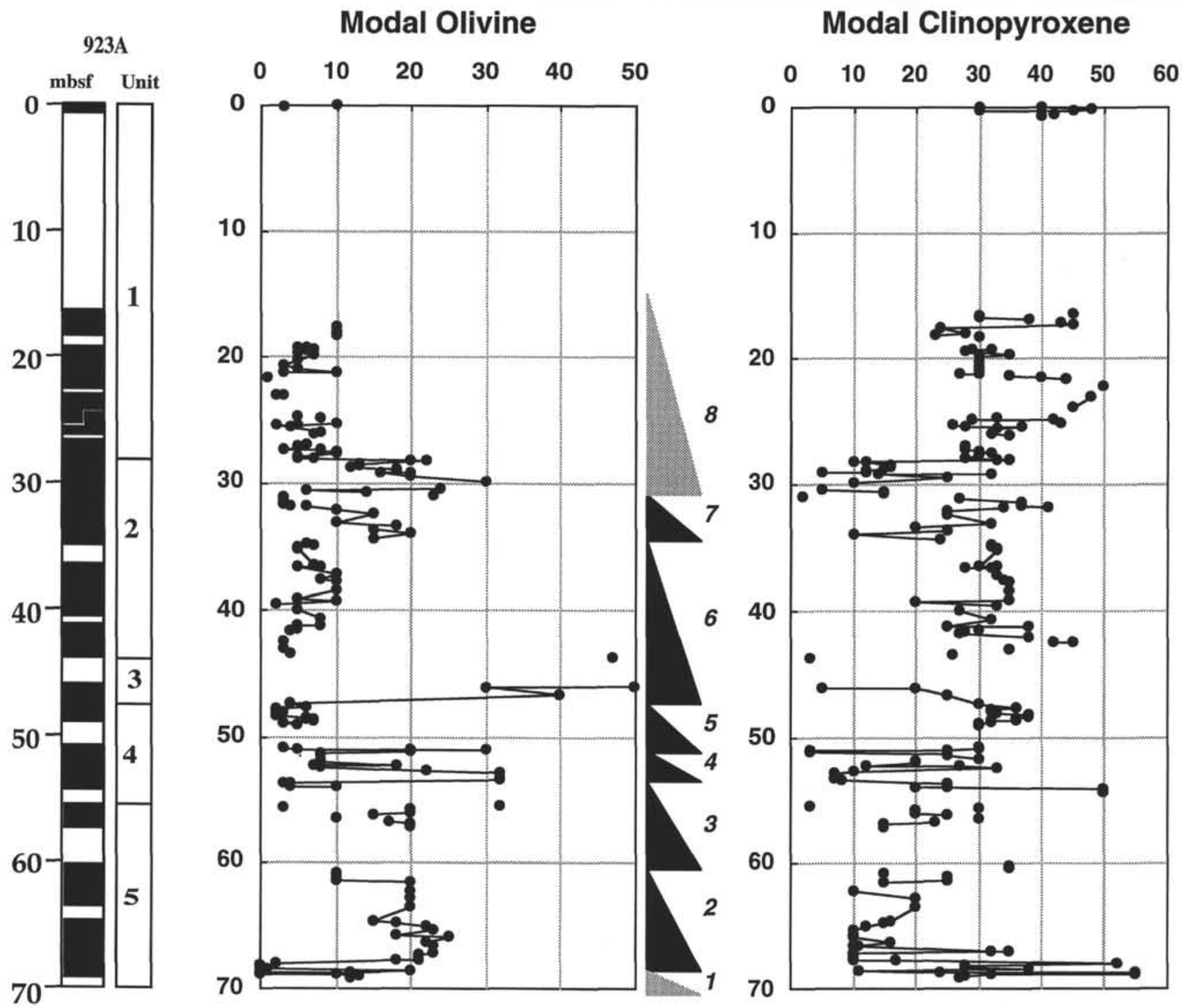

Figure 10. Plots of modal percentages of olivine and clinopyroxene versus depth in Hole 923A, showing relationship to textural cycles. See text for discussion.

OPERATIONS REPORT

The ODP Operations and Engineering personnel aboard *JOIDES Resolution* for Leg 153 were:

Operations Superintendent:	Tom Pettigrew
Development Engineer:	Leon Holloway
Schlumberger Engineer:	Steve Kittredge

ST. JOHN'S PORT CALL

Leg 153 of the Ocean Drilling Program (ODP) began at 0830 hr, 22 November 1993, with the first mooring line at Seabase Docks, St. John's, Newfoundland. The arrival of *JOIDES Resolution* in St. John's was two days ahead of schedule due to deteriorating weather in the Leg 152 operating area. With all Leg 153 personnel and equipment on board, *JOIDES Resolution* set sail with the last mooring line at 1530 hr, 27 November 1993.

ST. JOHN'S TO SITE 920 (Proposed Site MK-2)

The transit from St. John's, Newfoundland, to Site 920 (proposed site MK-2) covered 1500 nmi in 138.5 hr (5.8 days) at an average speed of 10.8 kt. During the transit a hard rock guide base (HRB) was moved into the moonpool area and partially assembled in anticipation of deployment at Site 920.

SITE 920

No seismic profiling was done on approach to Site 920. The vessel was navigated to the geographic coordinates for proposed site MK-2 where thrusters and hydrophones were lowered and final positioning was achieved in dynamic positioning (DP) mode. A positioning beacon was launched at 1212 hr, 3 December, initiating Site 920.

Once in DP mode a standard 9 drill collar rotary core barrel (RCB) bottom hole assembly (BHA) was made up and tripped to the seafloor. The vibration isolated TV (VIT), equipped with a releasable beacon, was lowered down the drill string for the seafloor survey. After approximately 8 hr of seafloor survey, a backup beacon was dropped from the VIT at 0700 hr, 4 December.

Hole 920A

After retrieving the VIT, Hole 920A was spudded at 0912 hr, 4 December. Seafloor depth was determined by drill pipe measurement to be 3339 mbrf (meters below rig floor) or 3328.3 mbsl (meters below sea level).

Hole 920A was cored to 3354 mbrf or 14 mbsf (meters below seafloor), recovering 0.84 m of core when the drill bit became plugged preventing circulation of the hole. The core barrel was retrieved, hole circulation reestablished, and another core barrel dropped. Upon landing of the second core barrel, it was determined the drill bit was still plugged preventing hole circulation.

The wireline became stuck when it was run in the hole in an attempt to unseat the core barrel to reestablish hole circulation. Repeated attempts to shear release the wireline running tool were unsuccessful. The Kinley Cutter was deployed, and the wireline severed just above the wireline sinker bar. After severing, the wireline and drill pipe were retrieved, ending Hole 920A at 2315 hr, 4 December.

Hole 920B

A 9 drill collar BHA was assembled and run in the hole. The VIT was deployed for an attempt at reentering Hole 920A. The BHA was landed on the seafloor and believed to be sitting on the edge of Hole 920A. The VIT was recovered to allow the drill string to be rotated in an effort to "walk" the bit into Hole 920A.

Rotating the drill string did not result in entering Hole 920A and thus Hole 920B was spudded at 2015 hr, 5 December. Hole 920B was initially drilled to 3353 mbrf (14 mbsf) so a pipe connection could be made without pulling the bit above the seafloor. Hole 920B was then cored 112.4 m to a total depth (TD) of 3465.5 mbrf (126.5 mbsf). Thirteen RCB cores were cut, recovering 44.57 m of core for a recovery percentage of 39.7%.

With 42.75 total rotating hr on the drill bit, a pipe trip was made for a bit change. A modified free fall funnel (FFF) was deployed before pulling out of the hole.

The bit cleared the FFF at 1328 hr, 8 December, and the ship was offset 10 m to the south for a jet test to determine the sediment thickness. The bit was jetted in 1.2 m with a flow rate of 250 gpm and 10 k lb weight on bit (WOB). The drill string was then retrieved.

A new 12 drill collar BHA, including a Hydrolex jar and 7-1/4" drill collar, was made up and deployed. The FFF at Hole 920B was reentered at 0800 hr, 9 December. The hole was reamed down 26 mbsf without fully entering the borehole.

The decision was made to trip out and deploy the hard rock guide base (HRB). Hole 920B ended when the bit cleared the seafloor at 1623 hr, 9 December.

Hole 920C

The HRB was picked up and run in the hole. The first landing proved to be on a 16° slope. Sonar indicated possibly more level terrain to the east, so the HRB was picked up and moved 5 m east. The tilt beacon, bulls eyes, and gravity indicators all indicated a 10° slope to the east-southeast. The HRB was positioned approximately 35 m east and 12 m north of Hole 920A/B. The seafloor depth was determined by drill pipe measurement to be 3343 mbrf (3332.2 mbsl). The drill string was released from the HRB and recovered.

A new BHA was made up consisting of a 17-1/2" bit and 12 drill collars. By the time the BHA was lowered to the seafloor, the HRB had settled, tilting an additional 2.6°. The HRB was reentered at 0325 hr, 11 December, and drilling commenced.

While drilling a 16 m deep hole, the HRB tilted an additional 1.3°. As the hole was being prepared for casing, the HRB tilted 1.9° more. At this time, the HRB angle was 15.8°. Since the HRB was equipped with a gimbal lock out feature, which stops movement of the reentry cone assembly once the HRB is landed, the reentry cone/hanger assembly was rotated 5.8° off vertical with settling of the HRB. Increased torque indicated the reentry cone assembly was binding on the BHA.

With the HRB effectively leaning on the BHA, the bit could not be worked back to the bottom of the hole. The decision was made to pull out of the hole and move the HRB. When the BHA was pulled out, the HRB tilted an additional 2.7°.

The 17-1/2" drilling BHA was recovered and replaced with the Dril Quip 20" CADA running tool. The CADA running tool was tripped to the seafloor and the HRB reentered at 1431 hr, 12 December.

As the running tool was being latched into the HRB, the reentry cone assembly toppled over. An attempt was made to straighten the reentry cone assembly and reenter it. However, since the landing point of the running tool is above the gimbal point and there was no stabilization of the running tool below the gimbal point, the reentry cone assembly toppled over again.

Since the running tool could not be latched into the HRB reentry cone assembly, the drill string was tripped out.

A 6-ft long, 17-$^{1}/_{2}$" stabilizer was fabricated from a 10-ft drill collar pup and 1 in.-thick steel plate. The stabilizer was made up below the CADA running tool and three drill collars were added above. The assembly was tripped to the seafloor and reentry attempted. On the third attempt the reentry cone assembly was righted and reentered. With the stabilizer in place, the reentry cone assembly stayed upright enabling the running tool to be latched in. The HRB was then recovered.

Hole 920D

A standard 12 collar RCB BHA was made up and run in the hole. Hole 920D was spudded at 0545 hr, 14 December, 10 m east of Hole 920B. Seafloor depth was determined by drill pipe measurement to be 3338 mbrf or 3327 mbsl.

Hole 920D was cored through RCB Core 20 to a depth of 3519.6 mbrf (181.6 mbsf) with only minor hole problems. However, while dropping RCB 21, the drill string became stuck by "ratchet" rocks lodged between the drill pipe tool joints. The drill string was eventually freed and RCB Cores 21 and 22 were cut to a depth of 3538.8 mbrf (200.8 mbsf) when the drill string became stuck again. Once free from the ratchet rocks, the drill string was worked to 3487 mbrf (149 mbsf) where all motion of the drill string was lost.

After working the stuck pipe for 12 hr, a severing charge was lowered down the pipe to 3342 mbrf (4 mbsf) and detonated. The severed drill string was pulled clear of the seafloor at 2012 hr, 19 December, ending Hole 920D.

SITE 920 TO SITE 921 (Proposed Site MK-1)

The 13.6-mi transit to Site 921 was made in DP mode while the drill string was being retrieved from Hole 920D.

SITE 921

A positioning beacon was deployed from *JOIDES Resolution* at 0620 hr, 20 December, initiating Site 921. A 16-hr seafloor survey was performed to locate level terrain for coring operations. A back-up positioning beacon was deployed from the VIT frame at 2235 hr, 20 December.

Hole 921A

An RCB BHA was made up and lowered to the seafloor and Hole 921A was spudded at 0200 hr, 21 December. Water depth was determined by drill pipe measurement to be 2488 mbrf (2477 mbsl). Two cores were cut to a depth of 2505.1 mbrf (17.1 mbsf), recovering 3.1 m. Constant hole fill and high erratic torque caused the hole to be abandoned at 0900 hr, 21 December, when the bit was pulled clear of the seafloor.

Hole 921B

The vessel was offset 30 m southeast of Hole 921A where Hole 921B was spudded at 0915 hr, 21 December. Drill pipe measurement indicated the water depth to be 2490 mbrf (2479 mbsl). While coring Hole 921A, an apparent fault zone was penetrated at 2514.5 mbrf (24.5 mbsf). The penetration rate doubled through the fault zone. Although high erratic torque and hole fill were present throughout the hole, they increased in the fault zone.

Hole 921B was cored 4 times to a depth of 2534.1 mbrf (44.1 mbsf), recovering 8.56 m. High erratic torque with hole fill eventually caused the hole to be abandoned. The bit was pulled clear of the seafloor at 1755 hr, 22 December, ending Hole 921B.

Hole 921C

The VIT was lowered to survey the immediate area around Hole 921B. The vessel was then offset 15 m southeast of Hole 921B and Hole 921C was spudded at 2235 hr, 22 December. The seafloor depth was determined by drill pipe measurement to be 2495 mbrf (2484 mbsl).

The first 6 m of Hole 921C cored at the rate of 3.5 m/hr. The penetration rate then dropped to less than 2 m/hr to a depth of 2534 m (39 mbsf) where a drilling break occurred. The penetration rate increased to 3.6 m/hr and the hole began to take fluid, as evidenced by low fluid levels in the drill string. High erratic torque and hole fill were observed to TD at 2548.4 mbrf (53.4 mbsf).

Hole 921C ended when the bit was pulled clear of the seafloor at 1150 hr, 24 December. Hole 921C was cored 7 times, penetrating 53.4 mbsf of fractured gabbroic material. Only 6.09 m of core was recovered for an 11.4% recovery rate.

Hole 921D

The BHA was round tripped for a bit change. Once the BHA was back on bottom, the VIT was deployed for a seafloor survey. After a 9-hr TV seafloor survey, Hole 921D was spudded at 0900 hr, 25 December, approximately 48 m east of Hole 921C. Drill pipe measurement indicated the water depth to be 2514 mbrf (2503 mbsl).

Hole 921D cored similarly to Hole 921C. The same apparent fault zone was encountered at 2534 mbrf (29.3 mbsf). As in Hole 921C, the penetration rate doubled, fluid was being lost to the formation, and high erratic torque with hole fill was encountered.

After cutting 5 RCB cores to a depth of 2562.6 mbrf (48.8 mbsf), recovering 6.16 m of core for a recovery rate of 12.7%, the decision was made to abandon the hole. Hole 921D ended at 1235 hr, 26 December, when the bit was pulled clear of the seafloor.

Hole 921E

The VIT was deployed once again for a seafloor survey. After 20 hr of surveying, the bit was placed in a small sediment pond on top of what appeared to be a large outcrop. The VIT was recovered and Hole 921E was spudded at 1201 hr, 27 December. Hole 921E is located approximately 200 m east of Hole 921D. The water depth was determined by drill pipe measurement to be 2456 mbrf (2444.9 mbsl).

The entire hole was cored with high erratic torque. Pump pressures slowly increased throughout the hole, occasionally dropping back to near normal levels. Frequent mud sweeps were used with only marginal success in reducing the pressure fluctuations and torquing.

The decision was made to abandon Hole 921E and move to another site. Hole 921E ended at 1827 hr, 29 December, as the bit cleared the seafloor. Nine cores were cut in Hole 921E to a depth of 2538.6 mbrf (82.6 mbsf), recovering 17.65 m.

SITE 921 to SITE 922 (Proposed Site MK-1)

As the drill string was being retrieved from Hole 921E, the vessel was offset in DP mode approximately 0.9 nmi to the south. A positioning beacon was dropped at 1720 hr, 29 December, initiating Site 922.

Site 922

Since none of the Site 921 pilot holes, Holes A, B, C, D, or E, indicated a favorable location for setting the HRB, the decision was made to investigate a new site. After reviewing *Nautile* dive tapes of the area, Site 922 was chosen.

Hole 922A

A new RCB BHA was made up and deployed. The VIT was then lowered down the drill string for a seafloor survey. After 21-1/2 hr of surveying, the bit was set on the seafloor to attempt spudding Hole 922A.

A jet test was performed at 350 gpm with 10 k lb WOB, resulting in virtually zero penetration. As the VIT was being retrieved in preparation for spudding the hole, the bit slid downhill 9.5 m.

The VIT was run back to bottom to inspect the BHA. The BHA was found intact and the bit was repositioned for spudding. Another jet test was performed with similar results. The VIT was then retrieved and Hole 922A was spudded at 2156 hr, 30 December.

The seafloor depth of Hole 922A was determined by drill pipe measurement to be 2612 mbrf (2600.9 mbsl). Hole 922A was cored 3 times to a total depth of 2626.6 mbrf (14.6 mbsf), recovering 9.23 m of metamorphosed gabbro. The overall penetration rate was approximately 0.3 m/hr.

The decision was made to pull out of the hole and set the HRB. The bit cleared the seafloor at 1612 hr, 1 January, ending Hole 922A

HRB Installation Attempt

The drill string was retrieved in preparation for deploying the HRB. The same HRB which was deployed at Hole 920C was picked up and lowered to the seafloor without incident.

The HRB was landed on the seafloor 13 times in 5-1/4 hr as the ship was offset between each landing. Each time the HRB was landed, a slope of greater than 25° was indicated. With ever increasing odds of damaging the HRB due to heave while landing, the decision was made to abort the landing and retrieve the HRB.

Hole 922B

After recovering the HRB, a new RCB BHA was made up. The BHA and VIT were lowered to the seafloor. A search was then made for Hole 922A with the intent of reentering and deepening it.

The first attempt at reentering what appeared to be Hole 922A was unsuccessful. After 2 hr of searching, another attempt was made at reentering what was believed to be Hole 922A. When the BHA landed on the seafloor without reentering the hole, the decision was made to spud Hole 922B at that location.

Hole 922B was spudded at 0900 hr, 3 January. The seafloor depth of Hole 922B was determined by drill pipe measurement to be 2612 mbrf (2600.8 mbsl).

The first core, Core 153-922B-1W, had to be cored to 14 mbsf before a drill pipe connection could be made without the bit heaving out of the hole. The hole was cored to 2649.4 mbrf (37.4 mbsf), recovering 9.53 m of gabbros. The penetration rate was 0.3 m/hr throughout most of the hole.

With 75.1 rotating hr on the bit, the decision was made to pull out of the hole for a bit change and attempt a reentry. Hole 922B was successfully reentered without a reentry funnel. However, when the hole was reamed to 12 mbsf, the BHA top sub box failed, leaving the outer core barrel assembly in the hole.

With the loss of the outer core barrel assembly, the hole could not be advanced. The drill string was pulled out of the hole, clearing the seafloor at 1215 hr, 7 January, ending Hole 922B.

SITE 922 TO SITE 923

As the drill string was being retrieved from Hole 922B, the Site 922 beacons were released and recovered. The vessel was then offset to a position approximately 150 m north of Hole 921E.

SITE 923

A new positioning beacon was dropped at 1730 hr, 7 January, initiating Site 923.

Hole 923A

A new RCB BHA was made up and run in the hole. The VIT was lowered down the drill string and an 8-hr seafloor survey began. After locating an appropriate spudding location, the bit was set on the seafloor and a jet test performed. The bit was jetted in 4.5 m while pumping 350 gpm at 450 psi with 10 k lb WOB.

While compensating the drill string, the VIT was retrieved and Hole 923A was spudded at 0950 hr, 8 January. The bit walked downhill approximately 4.5 m during the initial stages of spudding the hole. The bit finally came to rest and began making hole. The seafloor depth was determined by drill pipe measurement to be 2440 mbrf (2428.7 mbsl).

The hole cored very slowly at 0.3 m/hr. The lower 20 m of the hole required reaming with elevated circulating pressures and high erratic torque after each connection.

Following Core 153-923C-15R at 2504.7 m (64.7 mbsf), 2 hr was required reaming and cleaning the hole so coring operations could continue. The decision was made to cut one more core and then pull off bottom two singles before pulling the core barrel. The BHA had to be back reamed out of the hole. On each connection, high torque and high circulating pressures prevented recovery of the core barrel. Eventually the bit had to be pulled clear of the seafloor at 2258 hr, 12 January, ending Hole 923A and Site 923.

Hole 923A was cored 16 times to 2510 m (70 mbsf), recovering 40.03 m of gabbro for a 74% recovery rate.

SITE 923 TO SITE 924

The vessel was offset approximately 1.5 km to the east as the drill string was being recovered from Hole 923A. A positioning beacon was deployed at 0408 hr, 13 January, initiating Site 924.

SITE 924

Hole 924A

After recovering the drill string from Hole 923A, a new BHA was assembled. The BHA was tripped to the seafloor, followed by the VIT, and a seafloor survey was begun.

A spud site was located and the bit set on the seafloor. The bit was jetted in 0.5 m with 375 gpm and 8 k lb WOB. The seafloor depth was determined by drill pipe measurement to be 3170 mbrf (3158.7 mbsl). The VIT was retrieved and Hole 924A was spudded at 1724 hr, 13 January.

The hole was cored to 3180 mbrf (10 mbsf) where the drill collar immediately above the outer core barrel failed through the zip lift groove. The failure occurred 12 m above the seafloor at 0230 hr, 14 January, ending Hole 924A.

Hole 924B

A new BHA was made up and run in the hole, followed by the VIT. A 2-hr seafloor survey was carried out.

The vessel was offset 40 ft west of Hole 924A and the bit set on bottom. The bit was jetted 0.5 m at 375 gpm and 8 k lb WOB. As the VIT was being retrieved in preparation for spudding Hole 924B, the bit skidded downhill.

The bit was picked up clear of the seafloor as the VIT was run back to bottom. The vessel was offset 40 ft east of Hole 924A where the bit was set on bottom once again. A similar jet test was performed with similar results. The VIT was retrieved and Hole 924B was spudded at 2133 hr, 14 January. The seafloor depth was determined by drill pipe measurement to be 3176 mbrf (3164.7 mbsl).

Hole 924B was cored 3 times to a depth of 3206.8 mbrf (30.8 mbsf), recovering 2.69 m of gabbro. High torque and long reaming times, in conjunction with recovering small amounts of highly fractured material, resulted in the decision to abandon the hole.

The bit was pulled clear of the seafloor at 1135 hr, 16 January, ending Hole 924B.

Hole 924C

With the drill string already down, the VIT was deployed and a 2-hr seafloor survey was conducted. The first spud attempt resulted in the bit skidding downhill. Another spud site was chosen next to a cliff. The bit was set on bottom and a jet test performed. During the jet test, the bit cones could be seen as water was pumped between them. The vessel heaved and the bit skidded into a small crack nearby. The VIT was retrieved and Hole 924C was spudded at 1500 hr, 16 January.

The seafloor depth at Hole 924C was determined by drill pipe measurement to be 3177 mbrf (3165.7 mbsl). Hole 924C was cored 7 times to a depth of 3225.5 mbrf (48.5 mbsf), recovering 11.19 m of gabbro. Few hole problems were encountered.

With expiration of allotted coring time for the leg, the hole had to be abandoned. Hole 924C ended at 0500 hr, 20 January, when the bit cleared the rotary table.

SITE 924 TO BARBADOS

The transit from Site 924 began at 0542 hr, 20 January. The transit covered 1043 nmi in 97.3 hr at an average speed of 10.7 kt. *JOIDES Resolution* arrived in Bridgetown, Barbados, at 0600 hr, 20 January. The first line ashore was at 0730 hr, 20 January 1994, ending Leg 153.

OPERATIONS SUMMARY
Leg 153

Total Days (24 November 1993 - 24 January 1994)	63
Total Days in Port	5.3
Total Days Underway	9.9
Total Days on Site	47.8

Trip Time	9.8
Coring Time	26.9
Drilling Time	0.5
Reentry Time	6.4
Downhole Trouble Time	3.5
Other	0.7

Total Distance Traveled (nmi)	2543
Average Speed (kt)	10.75
Number of Sites	5
Number of Holes	15
Number of Reentries	1
Total Interval Cored (m)	798.3
Total Core Recovery (m)	261.1
Percent Core Recovered	32.7
Total Interval Drilled (m)	16
Total Penetration (m)	814.3
Maximum Penetration (m)	200.8
Maximum Water Depth (m from drilling datum)	3343
Minimum Water Depth (m from drilling datum)	2440

OCEAN DRILLING PROGRAM
SITE SUMMARY
LEG 153

HOLE	LATITUDE	LONGITUDE	WATER DEPTH (meters)	NUMBER OF CORES	INTERVAL CORED (meters)	CORE RECOVERED (meters)	PERCENT RECOVERED (percent)	DRILLED (meters)	TOTAL PENETRATION (meters)	TIME ON HOLE (hours)	TIME ON SITE (days)
920A	23*20.312N	45*01.038W	3339.0	1	14.0	0.84	6.0%	0.0	14.0	35.05	1.46
920B	23*20.312N	45*01.040W	3339.0	13	126.4	47.78	37.8%	0.0	126.4	113.25	4.72
920C	23*20.309N	45*01.033W	3343.0	0	0.0	0.00	0.0%	16.0	16.0	90.25	3.76
920D	23*20.322N	45*01.044W	3338.0	22	200.8	95.08	47.5%	0.0	200.8	155.17	6.47
		Site 920 TOTALS:		**36**	**341.2**	**143.70**	**42.1%**	**16.0**	**357.2**	**393.72**	**16.41**
921A	23*32.460N	45*1.870W	2488.0	2	17.1	3.10	18.1%	0.0	17.1	26.92	1.12
921B	23*32.478N	45*1.845W	2490.0	4	44.1	8.56	19.4%	0.0	44.1	32.67	1.36
921C	23*32.474N	45*1.832W	2495.0	7	53.4	6.09	11.4%	0.0	53.4	41.92	1.75
921D	23*32.446N	45*1.832W	2514.0	5	48.6	6.16	12.7%	0.0	48.6	48.75	2.03
921E	23*32.328N	45*1.878W	2456.0	9	82.6	17.65	21.4%	0.0	82.6	76.75	3.20
		Site 921 TOTALS:		**27**	**245.8**	**41.56**	**16.9%**	**0.0**	**245.8**	**227.01**	**9.46**
922A	23*31.362N	45*1.926W	2612.0	3	14.6	9.23	63.2%	0.0	14.6	70.87	2.95
922B	23*31.368N	45*1.926W	2612.0	5	37.4	11.95	32.0%	0.0	37.4	140.00	5.83
		Site 922 TOTALS:		**8**	**52.0**	**21.18**	**40.7%**	**0.0**	**52.0**	**210.87**	**8.79**
923A	23*32.556N	45*1.897W	2440.0	16	70.0	40.76	58.2%	0.0	70.0	130.65	5.44
		Site 923 TOTALS:		**16**	**70.0**	**40.76**	**58.2%**	**0.0**	**70.0**	**130.65**	**5.44**
924A	23*32.471N	45*0.881W	3170.0	0	10.0	0.00	0.0%	0.0	10.0	22.35	0.93
924B	23*32.470N	45*0.865W	3176.0	4	30.8	2.69	8.7%	0.0	30.8	57.08	2.38
924C	23*32.499N	45*0.866W	3177.0	7	48.5	11.19	23.1%	0.0	48.5	89.50	3.73
		Site 924 TOTALS:		**11**	**89.3**	**13.88**	**15.5%**	**0.0**	**89.3**	**168.93**	**7.04**
		LEG 153 TOTALS:		**98**	**798.30**	**261.08**	**32.7%**	**16.00**	**814.30**	**1131.18**	**47.13**

LEG 153
TOTAL TIME DISTRIBUTION

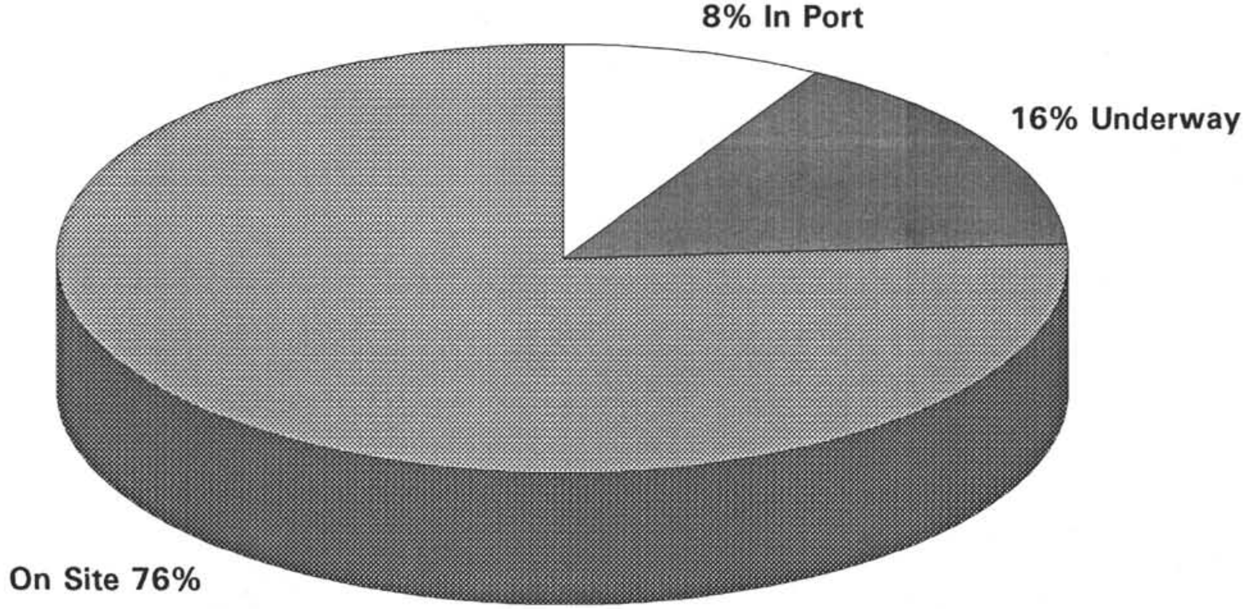

Total days of leg = 59.2

TECHNICAL REPORT

The following ODP Technical and Logistics personnel were aboard *JOIDES Resolution* for Leg 153 of the Ocean Drilling Program:

Laboratory Officer:	Burney Hamlin
Assistant Laboratory Officer, X-Ray:	"Kuro" Kuroki
Marine Laboratory Specialist/Curatorial Representative, Core Laboratory:	Erinn McCarty
Marine Computer Specialist/System Manager:	Joel Huddleston
Marine Computer Specialist/System Manager:	Edwin Garrett
Marine Laboratory Specialist/Yeoperson:	Jo Ribbens
Marine Laboratory Specialist/Chemistry:	Anne Pimmel
Marine Laboratory Specialist/Core Laboratory, Downhole Measurements:	Jaque Ledbetter
Marine Laboratory Specialist/Paleomagnetics:	Margaret Hastedt
Marine Laboratory Specialist/Photography:	Brad Cook
Marine Laboratory Specialist/Physical Properties:	Jon Lloyd
Marine Laboratory Specialist/Storekeeper, Thin Sections:	Tim Bronk
Marine Laboratory Specialist/Underway, Fantail:	Dwight Mossman
Marine Laboratory Specialist/X-Ray:	Wendy Autio
Marine Electronics Specialist:	Bill Stevens
Marine Electronics Specialist:	Mark Watson

INTRODUCTION

The Leg 153 technical staff assembled on 23 November 1993 in St. John's, Newfoundland. The *JOIDES Resolution* had docked two days early; severe Arctic storms and ice off the Greenland coast had necessitated the early termination of Leg 152. Cores and air freight had been offloaded prior to our arrival.

PORT CALL

The technical staff and scientists were transported to the ship on 24 November 1993 and crossover between the technical staffs commenced.

A technical representative familiar with our Ketema Doppler sonar system came aboard to inspect the installation and to isolate the reason for its poor performance in deep water mode. Suspect circuit boards were checked and found acceptable; the only fault located was the lack of a continuous air vent on the sea chest. An accumulation of air in the housing could possibly be creating internal reflections that would degrade the performance of the system.

Keith Carsten, from the Texas A&M Radiation Safety Office, surveyed our X-ray laboratory, the MST, the Faxitron, and the Schlumberger logging sources storage area. Radiation measurements were made while the units were in service. A two hour presentation on radiation physics, the use of various radiation counters, and safety was made to the technical staff. We were informed that this will probably be the last leg where radiation safety badges are issued to operators. Badges will still be issued to the Electronics Technicians who service the units. Keith Carsten will present a findings report to ODP.

Two representatives from Earl & Wright, naval architects, surveyed the ship to evaluate ODP's proposal to add a level to the ship house and to the core laboratory. After the tour, they obtained specific information from the Chief Engineer and Electrical Supervisor. Notes, sketches, measurements, photographs, and video tapes were made to document their visit and to serve as an onshore reference.

Problems associated with high chlorine levels in the water taken aboard on a previous St. John's port call were discussed with the Chief Engineer. The chlorine level was suitable for drinking water but was detrimental to the chemistry laboratory's reverse osmosis water purification system. A charcoal filter has now been added to the system to ensure there is not a repeat of the incident.

Two SUN workstations were installed in the underway laboratory by Staff Scientist Adam Klaus with Dennis Graham and Dwight Mossman in attendance. The SUN stations will be used to digitize and process seismic data, eventually replacing the existing MASSCOMP computers.

We took advantage of the availability of liquid helium in St. John's and obtained a dewar of the product to top off the cryogenic magnetometer; liquid helium is not locally available in Barbados where the next several port calls are planned. Assistance from 2G Enterprises, the fabricators of the cryogenic magnetometer, was not available during the Thanksgiving holiday but experienced scientists and our marine specialist were confident they could make the helium transfer. An ice blockage was discovered in the fill port that concluded the attempt. A fill for the second Barbados port call will be planned.

UNDERWAY

Navigation tapes were started as soon as we got underway but underway watches began as the ship left the Grand Banks, about a day out of port. The magnetometer sensor was deployed and the 12 kHz and 3.5 kHz depth recorders were turned on; no seismic gear was used.

Air was bled out of the doppler sonar housing with no noticeable improvement to deep-water performance. Raising and lowering the stem of the doppler sonar also produced no noticeable improvement.

Departing the drill sites, the seismic gear was deployed and seismic data were collected for one hour with the SUN workstation. Variations in pressure and flow rates were explored to optimize the use of the hose handler and the gun winches concurrently.

Expendable bathythermograph probes were dropped at six hour intervals; the data were relayed to NOAA via a satellite link.

BOTTOM SURVEYS

Over 110 hr of VHS video images were collected while surveying the selected sites for suitable drilling conditions of little sediment or slope.

CURATION

As on previous hard rocks legs, cores retrieved during Leg 153 were cut without liners. To recognize top from bottom, the bottoms of the cored rocks were marked with red wax markers as they were removed from the core barrel into pre-split liner halves. Steel-lined and chrome-plated barrels were alternated throughout the leg. Recovery was a percent or two better in the chrome-plated core liners.

During Leg 153, recovery was sufficient for the entire scientific party to obtain personal samples while staying within the ODP guidelines. Large samples, as for oversized thin sections, were carefully cut to limit the volume removed to half of the working half.

The cores recovered will stay on board until the next port call, after which they will be shipped to the Bremen Core Repository.

Bar code printers were introduced and used this leg and the bar code system will be implemented on the next leg.

Site 920 (proposed site MK-2) recovered peridotite. Sites 921 (proposed site MK-1), 922, 923, and 924 (proposed site MK-1) recovered gabbroic rocks.

CORE LABORATORY

The Branson sonic plastic welder was set up in the core splitting room as an alternate device for setting plastic dividers in the core liners. Although it worked well, many people are sensitive to the high frequency noise it generates; this noise is nearly inaudible to the operator when wearing ear protection. An acetone dip is still the preferred method for setting the plastic dividers, as it is very quick and the fumes are more tolerable than the noise to other personnel in the room when only a few dividers are set. The night crew did use the device enough to provide a comparison of the two methods for long term suitability.

A quartz 300 watt work light was used over the cutting table to aid alignment of the dark-colored rocks recovered.

The super saw with a masonry blade was used successfully to cut the long sections of core recovered. Some larger fractured pieces were held together with shrink wrap during cutting. Minicores were cut primarily with 1" stainless steel core drills and the ends were trimmed with the Leco Vari-cut precision saw.

A Vibra-lap device was introduced to the physical properties laboratory to polish thermal conductivity samples and the ends of the minicores. A steel jig was used with minicores and worked well with the Vibra-lap.

Maintenance was necessary on some of the sample cutting equipment. A bent spindle on one of the drill presses used with the core drills was replaced and later, a core drill collet was replaced. Bearings in the Felker saw arbor in the cutting room were replaced.

The MST was used to measure the density and the magnetic susceptibility of 223 sections. Magnetic susceptibility measurements, particularly in cores made up of peridotite, commonly exceeded the range of the instrument. Minicore volumes were determined using the pentapycnometer. The Hamilton Frame was used for ambient pressure horizontal compressional wave velocity measurements on minicores. Electrical resistivity measurements were made using the Wayne-Kerr analyzer. Thermal conductivity (TC) measurements were made using only TC box #1. More thermal conductivity needles were ordered for the TC box and some additional needles were found in the ET shop. There is an ongoing effort to consolidate all of the needles in the physical properties laboratory to facilitate storekeeping. Whenever the system stalled, it was a nuisance to reboot TC box #1 and the computer.

The paleomagnetics laboratory had a number of difficulties, partly because nearly every piece of equipment in the laboratory was used and chronic problems resurfaced. Most were minor and easily rectified.

The cryogenic magnetometer measured the fields in 250 half sections and 276 discrete or minicore samples. The Y-axis electronics seems to be deteriorating, making measurements troublesome. Opening and closing the shield for access is becoming a nuisance. The problems were intermittent, however, and measurements continued to be made. There is more electrical noise than in the past year and it is more time consuming to tune the X, Y, and Z axis squids. Troubleshooting has not yet resolved some difficulties despite correspondence with 2G Enterprises.

Several software utilities were modified to better accommodate high-intensity values.

No downhole tools were deployed on this leg, although the sonic core monitor was prepared for use and bench-tested at the request of the scientific party. Software problems encountered previously with the Tensor tool software were investigated and diagnosed as a timing problem; this problem was corrected.

Cross training was initiated between the marine specialists in the cryogenic magnetometer laboratory, Margaret Hastedt, and physical properties laboratory, Jon Lloyd. The many instruments in operation and number of files generated in the physical properties laboratory will make this an ongoing project.

CHEMISTRY LABORATORY

Little support was requested from the chemistry laboratory other than providing hydrogen and carbon values with the CHNS analyzer. These values are used by the XRF laboratory to calculate water and carbon dioxide losses during XRF sample ignition.

The hydrogen generators required maintenance, as the cells were going dry; failure of a flapper valve in the cell was indicated. Subsequent catalyst release caused the cell to fail. A replacement hydrogen unit and a spare cell were ordered.

A Barnstead Ropure water system was installed over the chemistry laboratory's starboard sink. The nanopure water unit was moved and attached to the Barnstead Ropure unit and the combination produces very good quality water.

Other laboratory instruments were tested occasionally to ensure operability, but not used specifically for analytical purposes.

A rain gutter was welded over the emergency escape door from the chemistry laboratory. The door gasket was also rotated in an effort to eliminate leakage.

X-RAY LABORATORY

The XRF was used extensively to analyze the recovered rocks. Two calibrations were performed on the XRF, one for each of the rock types recovered. The unit ran well with few problems. Some difficulties were encountered with sample preparation. Poor agreement between duplicate fused XRF beads was traced back to the Claisse Fluxer, and there was an observed difference in the trace element abundances for ignited vs unignited ultramafic rocks. Some drift problems were encountered after a P-10 gas bottle change and it is recommended that all hard rock legs start with a full bottle of P-10 gas.

Some software problems were resolved and new ones encountered. As the cruise progressed, totals were creeping over 100%, generating concern that the laboratory standards were old and beginning to break down. This possibility is being investigated. Two inter-laboratory standards were prepared from drill cuttings and rocks caught in a bit.

Mechanical problems with the XRF occurred less frequently than on previous legs. Sample changer jamming was finally eliminated by careful adjustment of the microswitches and lift assembly. Two vacuum pumps were rebuilt.

The Claisse Fluxer was unstable during this cruise and was eventually disassembled and rebuilt. The problem was attributed to uneven and inconsistent flame temperatures which affect bead characteristics and thus analytical precision. Higher temperatures were attained after the cleaned parts were reassembled but the problem of different and variable temperatures between the pair of burners was not resolved.

A new bench top freeze drier was added to the laboratory's equipment inventory; it is efficient and convenient.

Jaque Ledbetter worked with Wendy Autio to become acquainted with the laboratory sample preparation procedures and instruments.

The XRD was used primarily to identify vein minerals for the scientific party. A utility program was written to add flexibility to the plotting routines used to graph the data.

THIN SECTION LABORATORY

Of the more than 300 thin sections made during this leg, 27 were oversized and all were polished. Bearings were replaced on the Buehler lap wheel and a vacuum pump was rebuilt. The Logitech CS-10 cut-off saw and various spare parts were returned to ODP for onshore use or surplus. The Petro-thin cut-off saw was used for all thin section preparation. A Logitech LP-30 lapping jig was disassembled, cleaned, lubricated, and lapped true again.

PALEONTOLOGY LABORATORY

There was no paleontological work conducted during this leg. However, the shatter box and Spex mill were moved from the X-ray laboratory sample preparation area into the paleontology laboratory.

A water spray hose was added to the sample washing sink to aid sieving. A small, salvaged metal cabinet was modified to accommodate the reference slides and specialized small tools. The large reference catalogs remain in the Tech Office. The hot and cold water lines were reversed at the sink in the HF preparation area, correcting a previous oversight.

COMPUTER SERVICE

The VAX 11/750's were shut down for the last time and were prepared for shipment back to ODP. The μVAX 3500's have assumed all functions of the original, and physically much larger, system. The additional memory installed in the μVAX's during the last leg allowed ane increase in memory allocation to many ODP standard programs. Memory allocation schemes for the network and batch software still need improvement. The system functioned well during this cruise.

Tests were conducted on the new EXCEL macro, which adds depth information to spreadsheets. One minor modification increased its speed. However, the scientists chose to save data in an alternate format.

During this leg, the Macintosh 4th Dimension database, ROCKY, was tested for the first time. This database utilizes a MAC IIx as a multi-user server. As the record file grew to more than 500 entries, response time was quite slow. This problem was exacerbated by multiple users. Core data could be obtained but it was incomplete and poorly formatted. A faster computer should be considered. The problem will be rectified onshore.

Minimal use was made of the new MAC color scanner which was installed during the last leg. The current hardware configuration (a Macintosh IIx) lacks sufficient memory to efficiently deal with the large electronic files generated. Coprocessor speed is also inadequate as it can take more than 30 minutes to save a scanned document, diminishing the utility of the high resolution capabilities of the new system. A faster computer, such as a MAC Quadra with 32 Mbytes of memory, is recommended.

Assorted failed components are being returned for repair or replacement. One vendor's PC's have a problem with cache memory failures. There are no spare MAC compatible monitors on board.

PHOTOGRAPHY LABORATORY

The majority of the camera and laboratory processing equipment functioned well. The Kreonite film processor was partially overhauled with some gears and roller socks replaced. The chiller in the Kreonite deep tank sink failed and a new motor was installed. A new, larger film drying cabinet replaced an older product.

MICROSCOPES

Few microscope problems were noted. The instruments were set up according to a poll of the scientific party which identified common requirements. One damaged ocular head will be returned for repair.

ELECTRONICS SHOP

Most laboratories required attention from the ET's. Both XEROX copiers, the cryogenic magnetometer, the XRF, the hydrogen generators, the MST optical encoder connector, and thermal conductivity box components all required repair. Assistance was provided during installation of the bar code printers. A fan motor was replaced in the air tempering unit of the processor in the photography laboratory.

A new desk was installed on the Bridge to accommodate the weather monitoring system computer. After rebooting the system, no weather maps could be received. A mistake made during setup of one of the files provided local instead of the desired UTC time. Also a small speaker used to monitor audible signals from satellites required battery power. These problems were rectified by midway through the leg.

STOREKEEPING

The oncoming shipment in St. John's was large, but no problems were encountered during loading. Full stocks of bulk consumables to support the expected high recovery during Leg 154 were received. The casing hold was full, making it difficult to set up K-boxes for Leg 153's shipment. Cold weather clothing and equipment from the last two legs were collected and are being returned to ODP for cleaning and storage. Ship stores has exceeded the storage capacity of the closet; the overflow is locked in the 2nd look laboratory.

SPECIAL PROJECTS

The physical properties laboratory bench was extended and a smaller stainless steel sink was installed at the aft end of the bench. This provides room to lay out sections of core across the bench when needed.

A paper titled *Introduction To Shipboard Organic Chemistry* was prepared by our chemist for Marine Specialists, Shipboard Scientists, and Operations Managers. This paper, which describes various hydrocarbon monitoring procedures used on board *JOIDES Resolution,* will be reviewed onshore.

A program called LAPOTIN V.1 was used to model ADARA heat flow data collected on Leg 151. Our downhole tools specialist believes it can be a valuable time saver as it may reduce the number of heat flow runs requested. The program predicts the thermal (hydrocarbon) maturity of sediment based on the thermal gradient and burial depth. Her study and the program will be reviewed onshore.

The 10 horsepower (HP) hydraulic power pack that powers the gun booms and winches was replaced with a 30 HP unit. This will allow the use of hydraulic hose handlers which reduces the number of people needed to retrieve the seismic gear. SEDCO personnel handled installation of the new unit.

A push-button lock was installed on the door to the 2nd look laboratory to alleviate the recurring problem of misplaced keys.

SAFETY

The METS team members selected their appropriately sized fire gear and stored it in mesh bags for better organization and ease of carrying to the staging area.

A new fire drill procedure was introduced during this leg in order to reduce response time; participants are instructed to go directly to the scene of the fire.

The hazardous spill kits located in barrels at the hold level of the lab stack stairwell were transferred to large yellow plastic bins on wheels. This will protect the products from water and make them easier to transport in the event of a chemical spill. Eye and body wash stations were installed on the mezzanine level where acids are stored.

The PVC surface on the core laboratory splitting room Felker saw was replaced. Vibration of some of the cores being cut contributed to bent saw blades and sore fingers.

Angle iron was welded underneath a small section of fibergrate decking to provide additional support.

LEG 153 LABORATORY STATISTICS

GENERAL:

Sites:	5
Holes:	15
Meters Drilled:	800.5
Meters Cored:	784.5
Meters Recovered:	254.7
Time on Site (days)	47.1
Number of Cores	101
Number of Samples:	2608
Number of Core Boxes:	52

Final positions for Leg 153:

Hole 920A:	23° 20.312 N; 45°01.038W	Hole 920B:	23° 20.312 N; 45°01.040W
Hole 920C:	23° 20.309 N; 45°01.033W	Hole 920D:	23° 20.322 N; 45°01.044W
Hole 921A:	23° 32.460 N; 45°01.870W	Hole 921B:	23° 32.478 N; 45°01.845W
Hole 921C:	23° 32.474 N; 45°01.832W	Hole 921D:	23° 32.446 N; 45°01.832W
Hole 921E:	23° 32.328 N; 45°01.878W		
Hole 922A:	23° 31.362 N; 45° 01.926W	Hole 922B:	23° 31.368 N; 45° 01.926W
Hole 923A:	23° 32.556 N; 45° 01.897W		
Hole 924A:	23° 32.471 N; 45° 00.881W	Hole 924B:	23° 32.470 N; 45° 00.865W
Hole 924C:	23° 32.499 N; 45° 00.866W		

ANALYSIS:

Magnetics:	Half section measurements	250
	Discrete measurements:	276
	Kappabridge	276
Physical Properties:	Index properties:	211
	Velocity	211
	Resistivity	211
	Therm con	172
	MST	223
Chemistry:	CNHS	106
X-ray:	XRD	54
	XRF	106
Thin Sections:		304

UNDERWAY GEOPHYSICS:

Total Transit (nmi):	2754
Bathymetry (nmi):	2274
Magnetics (nmi):	2274
XBT's (nmi):	34